55. Molecular Geometries by the Extended-*Hückel* Molecular Orbital Method II: Hydrocarbons and Organic Molecules Containing O, N, and S

by **Martin Brändle** and **Gion Calzaferri***

Institute for Inorganic and Physical Chemistry, University of Bern, Freiestrasse 3, CH–3000 Bern 9

(23.XI.92)

Bond lengths and bond angles of hydrocarbons and of organic molecules containing oxygen, nitrogen, and sulfur have been investigated by the extended-*Hückel* method in its improved ASED (atom superposition and electron delocalization) form. We have examined in detail bond lengths and bond angles of hydrocarbons – aliphatic, conjugated, rings, and aromatic – and we have also studied reaction enthalpies. Both properties can be calculated resonably well, if a small adjustment of the parameter κ in the distance dependent *Wolfsberg-Helmholz* formula is accepted. We have also found that moderate contraction of the usually applied 2s-oxygen, the 2s-nitrogen, and the 3s-sulfur *Slater* exponents is sufficient to obtain astonishingly good geometries for important classes of organic molecules containing these elements. The three-membered rings $(CH_2)_2X$ (X = CH_2, NH, O, and S) which have attracted much interest and stimulated theoretical studies have been investigated, and we have found that their geometries can be reproduced nicely. It is important that geometry calculation of the investigated molecules can be carried out *without losing transparency* and *well established prediction capabilities of the original EHMO procedure*. The extended-*Hückel* method in its improved ASED form is, therefore, a useful tool for combining the information of the EHMO results with good geometry calculation.

1. Introduction. – *Roald Hoffmann* has helped chemists to understand the structure of organic and inorganic molecules and solids, the reactivity of molecules, and interactions of molecules on surfaces in a series of brilliant papers of which we mention only a few [1–10]. Most of these studies are based on extended-*Hückel*-type calculations [2]. Application of the extended-*Hückel* procedure by many other authors has influenced the contemporary way of reasoning in different fields, see *e.g.* [11–24]. In addition to its transparency, one of the most fascinating aspects of this method is that it can be applied to study molecules, clusters, solids, and the interaction of molecules on surfaces. It has always been known that the EHMO method in its original form does not correctly include electrostatic interaction and, therefore, often fails to yield good potential-energy curves for stretching modes. *Anderson* and *Hoffmann* have shown how this deficiency can be overcome by adding a two-body electrostatic correction term, applying the *Hellmann-Feynmann* theorem [19]. To derive the two-body electrostatic interaction energy, the exact electronic charge density $\rho(R_\alpha, r)$ for a diatomic molecule $\alpha-\beta$ is written as

$$\rho(R_\alpha, r) = \rho_\beta(r) + \rho_\alpha(R_\alpha - r) + \rho_{\mathrm{NPF}}(R_\alpha, r) \tag{1}$$

where the origin of the coordinate system is on nucleus β. $\rho_\beta(r)$ and $\rho_\alpha(R_\alpha - r)$ are atomic charge densities, centred on nucleus β and nucleus α. R and r are electron and nuclear coordinates, respectively. These densities are computed by using the same *Slater* orbitals as those in the extended-*Hückel* calculation. $\rho_{\mathrm{NPF}}(R_\alpha, r)$ is the 'non-perfectly-following'

correction to the atomic charge densities which makes *Eqn. 1* exact. The energy $E(R)$ is expressed as the sum of the electrostatic two-body correction $E_{\alpha\beta}(R)$ and the extended-*Hückel* binding energy $\Delta E_{\text{EHMO}}(R)$. $\rho_{\text{NPI}}(R_\alpha, r)$ can be estimated from the resulting wavefunctions.

$$E(R) = E_{\alpha\beta}(R) + \Delta E_{\text{EHMO}}(R) \tag{2}$$

The extended-*Hückel* binding energy $\Delta E_{\text{EHMO}}(R)$ is expressed as

$$\Delta E_{\text{EHMO}}(R) = E_{\text{EHMO}}(R) - \sum_{\text{s}} b_{\text{s}}^0 E_{\text{s}}^0 \tag{3}$$

where $\sum_{\text{s}} b_{\text{s}}^0 E_{\text{s}}^0$ is the sum of atomic valence orbital ionization potentials, each of them times the orbital occupation number b_{s}^0.

Encouraged by the results of *Anderson*'s ASED-MO (atom superposition and electron delocalization) theory on diatomic molecules [20], we have adopted it, have eliminated some of the deficiencies encountered, and we have generalized it for polyatomic molecules [21]. Some features of this approach have been discussed in a recent study of the electronic structure and reactivity of octasilasesquioxanes $X_8Si_8O_{12}$ [22]. It was shown that reliable bond distances can be calculated without losing the transparency of the original extended-*Hückel* method. A discussion of properties of M(II,d^6)-4′-phenylpyridine complexes [23] and also a study of the first excited states of DMABN [24] based on this computing procedure have led to the same conclusion.

After the appearance of the first paper on molecular geometries by the EHMO method [21a], hereafter referred to as I, one of the authors (*G. C.*) was asked on several occasions, if the modification of *Anderson*'s ASED-MO method can be used as a tool for molecular modeling of neutral molecules, thus combining the information of the EHMO results with good geometry prediction. From the beginning, we hoped that this might become a possibility at least for many classes of molecules.

The first very large class of molecules to try are the hydrocarbons. Provided that the difference of single, double, and triple bonds can be described correctly, they should work. We have, therefore, investigated in detail bond lengths and bond angles of this class of molecules, and we have also studied reaction enthalpies. Both properties can be calculated reasonably well, if a small adjustment of the parameter κ in the distance dependent *Wolfsberg-Helmholz* formula (*Eqn. 5*) is accepted. The number of molecules of interest can be extended enormously, if the elements oxygen, nitrogen, and sulfur are included. For this reason, geometry calculations of a number of organic molecules containing these elements have been carried out and are explained. We will show that minor modification of the 2s-oxygen, the 2s-nitrogen, and the 3s-sulfur *Slater* exponents is sufficient to obtain astonishingly good geometries for important classes of molecules. The aim of this paper is, however, not to present an optimized parameter set, but to discuss possibilities of the method, potential applications and interpretations.

A discussion of molecular modeling by means of the EHMO theory makes sense only, if the two-body electrostatic energy is included [21]. This can be understood by looking at the energy dependence of the C–C stretching mode of ethine in *Fig. 1* as an example. The extended-*Hückel* binding energy $\Delta E_{\text{EHMO}}(R)$ decreases in both cases with decreasing bond distance. Addition of the electrostatic two-body correction $E_{\text{Rep}}(R)$ (*Eqn. 6*) leads to the satisfactory solid curve $E(R)$, thus repairing the deficiencies of the extended-*Hückel* method in calculating bond distances.

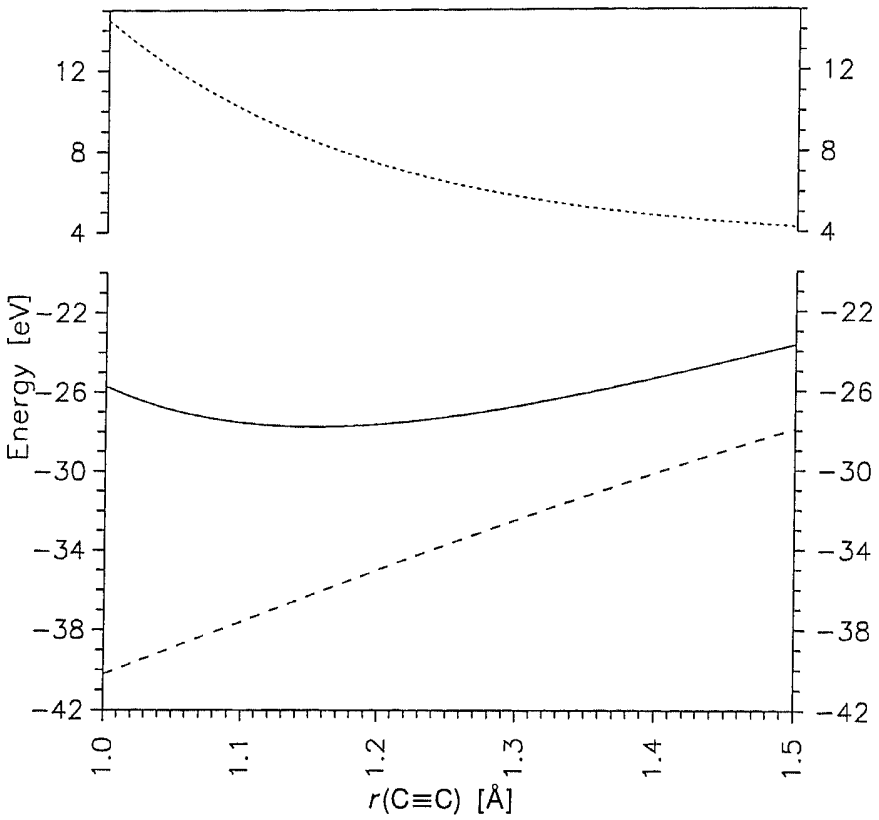

Fig. 1. *Energy of ethine as a function of the internuclear distance* r *(C ≡ C).* (· · ·): Two-body interaction E_{Rep}, (——): total energy $E_{tot} = \Delta E_{EHMO} + E_{Rep}$, (----): extended-*Hückel* binding energy ΔE_{EHMO}.

2. Method. – Calculations were carried out by the extended-*Hückel* method [2], with the parameters collected in *Table 1*. If not otherwise stated, parameters were kept constant during all the calculations. *Mulliken* population analysis was applied [25], and the *Coulomb* integrals H_{ii} were taken from the literature in case of the hydrocarbons [2]. For the O- and S-containing compounds, they were obtained by charge iteration [12] on H_2O and H_2S, respectively, at equilibrium geometries with the parameters from [11]. The off-diagonal elements were calculated as [26]

$$H_{ij} = \frac{1}{2} K S_{ij} (H_{ii} + H_{jj}) \tag{4}$$

For the *Wolfsberg-Helmholz* parameter, we use the weighted formula [27] in its distance-dependent form [21].

$$K = 1 + k e^{-\delta(R - d_0)} \text{ with } k = \kappa + \Delta^2 - \Delta^4 \kappa \text{ and } \Delta = \frac{H_{ii} - H_{jj}}{H_{ii} + H_{jj}} \tag{5}$$

Table 1. Slater *Parameters and* Coulomb *Integrals*

Element	n	ζ_{ns}	H_{ss}/eV	ζ_{np}	H_{pp}/eV
H	1	1.300	−13.60		
C	2	1.71	−21.4	1.625	−11.4
N	2	2.14	−26.0	1.95	−13.4
O	2	2.575	−28.20	2.225	−12.40
S	3	2.283	−20.48	1.817	−11.43

In this equation κ affects the value of K at $R = d_0$, and δ determines how fast K decreases with increasing bond distance. d_0 is equal to the sum of the orbital radii and is calculated from the *Slater* exponents. If not otherwise stated, κ was 1.0 and $\delta = 0.35$ Å^{-1}. The value $K = 1.75$ was originally chosen as a reasonable compromise between the desire to match the experimental barrier in ethane, and the necessity to work in a region where populations are stable [2]. Addition of the two-body correction to the stabilization energy as explained in [21a] shifts the minimum of $E(R)$ to longer distances than that of the original $\Delta E_{\text{EHMO}}(R)$, thus a larger K value at $R = d_0$ is generally needed. The two-body correction $E_{\alpha\beta}(R)$ for polyatomic molecules is calculated as a sum over all atom-atom interactions. Since it is always repulsive, we denote it as E_{Rep} and number the atoms with the indices α and β:

$$E_{\text{Rep}} = \frac{1}{2}\sum_{\alpha,\beta} E_{\text{Rep}_{\alpha,\beta}} \tag{6}$$

The extended-*Hückel* binding energy ΔE_{EHMO} and the electrostatic two-body correction E_{Rep} can be split into their atom contributions for further analysis. E_{EHMO} is expressed as sum over the one electron states E_i times the occupation numbers b_i

$$E_{\text{EHMO}} = \sum_i b_i E_i \tag{7}$$

$$E_i = \sum_{\alpha_s} c_{i,\alpha_s}^2 H_{\alpha_s,\alpha_s} + 2 \sum_{\alpha_s < \beta_t} c_{i,\alpha_s} c_{i,\beta_t} H_{\alpha_s,\beta_t} \tag{8}$$

with α, β denoting atom indices and s, t their corresponding atomic orbital indices. Partitioning is expressed by the energy matrix:

$$E_{\text{EHMO}_{\alpha_s,\beta_t}} = a \sum_i b_i c_{i,\alpha_s} c_{i,\beta_t} H_{\alpha_s,\beta_t} \quad (a = 2 \quad \text{if} \quad \alpha_s \neq \beta_t, \text{ else } a = 1) \tag{9}$$

Dividing the energy matrix elements equally between two atoms, we can write:

$$E_{\text{EHMO}_\alpha} = \sum_s E_{\text{EHMO}_{\alpha_s,\alpha_s}} + \frac{1}{2}\sum_{s<t} E_{\text{EHMO}_{\alpha_s,\beta_t}} \tag{10}$$

The stabilization energy $\Delta E_{\text{EHMO}_\alpha}$ each atom α gains in the molecule with respect to its isolated atom valence state is equal to the difference of E_{EHMO_α} and the sum of the valence orbital ionization potential E_s^0 each times the orbital occupation number b_s^0.

$$\Delta E_{\text{EHMO}_\alpha} = E_{\text{EHMO}_\alpha} - \sum_s b_s^0 E_s^0 \tag{11}$$

A similar partitioning of the electrostatic two-body repulsion energy E_{Rep} makes sense, in which each atom contributes E_{Rep_α} defined as follows:

$$E_{\text{Rep}_\alpha} = \frac{1}{4}\sum_\beta E_{\text{Rep}_{\alpha,\beta}} \tag{12}$$

The total energy gain E_α of each atom in the molecule is expressed as sum of the stabilization $\Delta E_{\text{EHMO}_\alpha}$ and the repulsion E_{Rep_α}, by analogy with *Eqn. 2*:

$$E_\alpha = E_{\text{Rep}_\alpha} + \Delta E_{\text{EHMO}_\alpha} \tag{13}$$

3. Hydrocarbons. – Let us compare calculated and experimental geometries of representative hydrocarbons – aliphatic, conjugated, rings, and aromatic – in *Table 2*. We refer

Table 2. *Comparison of Experimental and Calculated C–C and C–H Distances of Some Hydrocarbons* [Å]

Molecule	C–C		C=C		C≡C		–C–H		=C–H		≡C–H	
	Exper.	Calc.	Exper.	Calc.	Exper.	Calc.	Exper.	Calc.	Exper.	Calc.	Exper.	Calc.
CH_4							1.094	1.08				
$CH_3–CH_3$	1.533	1.64					1.111	1.07				
$CH_2=CH_2$			1.339	1.33					1.085	1.07		
Propene	1.501	1.52	1.336	1.33			1.09[a])	1.08	1.09[b])	1.06		
s-*trans*-Butadiene	1.465	1.52	1.345	1.33					1.108[b])	1.07		
H–C≡C–H					1.203	1.15					1.061	1.04
Propyne	1.458	1.53			1.207	1.15	1.112	1.08			1.060	1.04
Cyclopropane	1.512	1.58					1.083	1.05				
Cyclopropene	1.515	1.60	1.300	1.26			1.087	1.05	1.070	1.04		
Cyclobutadiene	1.527[c])	1.70	1.441	1.31					–	1.05		
Cyclohexene	1.53	1.61[d])	1.34	1.35			1.10	1.07	1.09	1.06		
	1.51[e])	1.57										
Benzene			1.396	1.41			1.083	1.06				
Styrene	1.475[f])	1.55	1.34[f])	1.33					1.09[d])	1.06		
(*E*)-Stilbene[g])	1.48[h])	1.54	1.33[h])	1.34					1.095[d])	1.05		

[a]) Mean value of all –C–H bonds.
[b]) Mean value of all =C–H bonds.
[c]) Taken from X-ray structure determination of tetra(*tert*-butyl)cyclobutadiene at 123 K [31].
[d]) Mean value.
[e]) Bond adjacent to C=C.
[f]) *Ab initio* values with empirical corrections [32].
[g]) Assumed to be planar.
[h]) See [33].

to the experimental gas-phase geometries reported in [28] if not otherwise stated. As a general trend, the calculated C–C bonds are too long, deviations ranging from 0.02 Å in case of propene to 0.11 Å in ethane. The discrepancy for cyclobutadiene is larger, but in this case the experimental value is also uncertain. Calculated C=C bond lengths differ from the experimental values by less than 0.02 Å, again with the exception of cyclobutadiene which is distorted by first-order *Jahn-Teller* [29], an effect that comes out nicely. The calculated C≡C bonds are too short by less than 0.06 Å, and the C–H bond lengths are only slightly too short. The largest difference encountered between calculated and experimental bond lengths is generally less than 0.1 Å. We conclude that the agreement between experimental and calculated values is good, in view of the fact that a non-optimized single parameter set has been used.

Apart from considering bond lengths and bond angles, it is relevant to study the energy dependence along internal coordinates. We do this for the ethane molecule, starting with the total energy surface in *Fig. 2a* where the r(C–C) and the r(C–H)

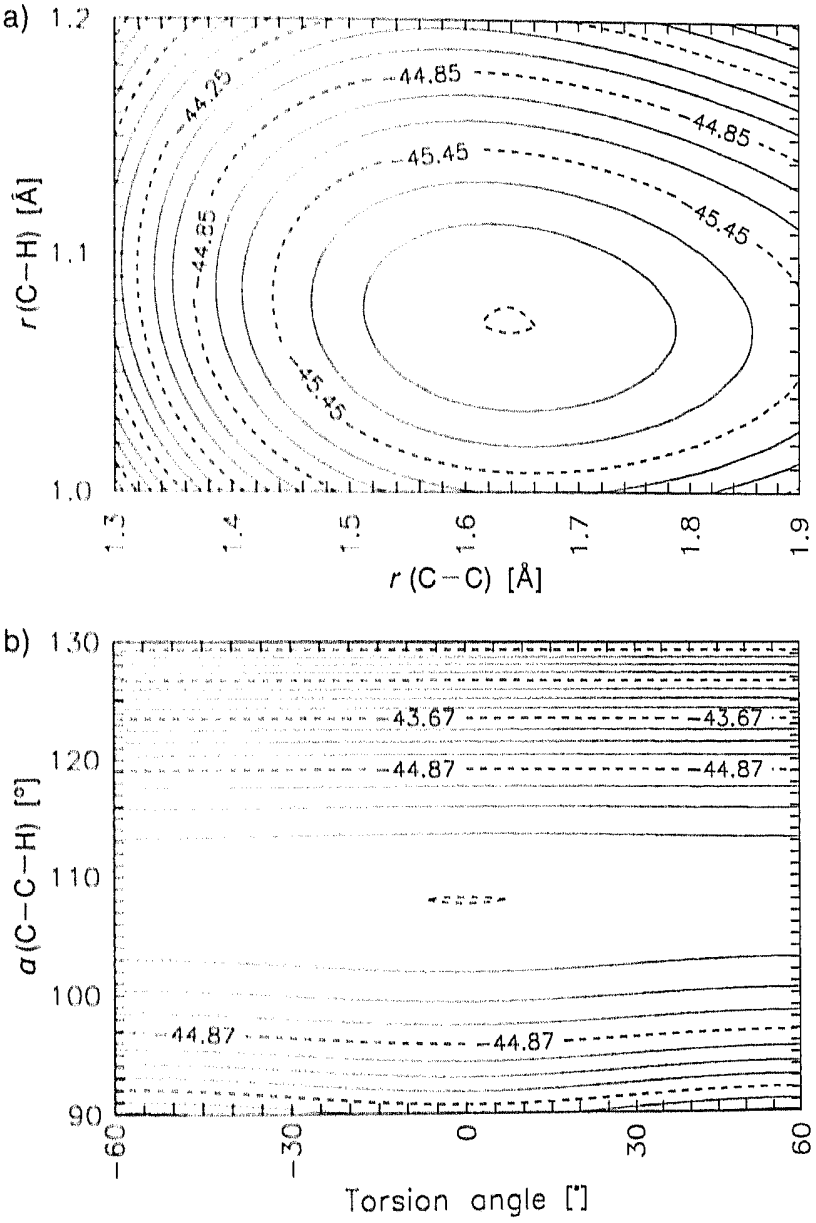

Fig. 2. *Potential surface* E_{tot} [eV] *of ethane for* a) *the symmetrical C–C and C–H stretching motion and* b) *for the Me group torsion and C–H binding*

coordinates are varied. The shape of the hypersurface indicates only weak coupling between the C–C and the C–H stretching modes. This is correct, as we know from IR spectroscopy. The behavior of the two modes illustrated in *Fig. 2b* is also correct. The torsional motion of the Me groups around the C–C bond and the bending angle α(C–C–H) are independent from each other. The staggered conformation with a torsional angle of 0° at α(C–C–H) = 108° (experimental 111.6°) is the most stable one.

Bond angles are usually well described by the EHMO method without the repulsion term, and one may ask how E_{Rep} varies along these modes. To answer this, we show in *Fig. 3a* a cut along the torsional path and compare the repulsion, the total and the stabilization energy. Obviously E_{Rep} does not influence torsion in this molecule. The H-atoms are too far apart so that the repulsion energy is not influenced by this coordinate. The height of the barrier along E_{tot} and along ΔE_{EHMO} is about the same 6 kJ/mol. Since the product of the *Boltzmann* constant k_B and the room temperature is 2.5 kJ/mol, the calculation simulates free rotation at ambient temperature. The experimental barrier has been reported as 12 kJ/mol and the torsion vibrational frequency is 290 cm^{-1} [30]. From this very low energy barrier discussion, we now move to the torsional mode of a vinyl group around the C–C bond of buta-1,3-diene (**I**). We again compare the repulsion, the total and the stabilization energy in *Fig. 3b*. E_{Rep} remains nearly constant for the same reason as before. A small rise is observed in the *cis*-conformer due to the interaction of the hydrogens in positions 1 and 4. It turns out that the *trans*-conformation is more stable than *cis* by 8 kJ/mol which is close to the experimental value of 10.4 kJ/mol [34]. They are separated by an activation barrier of 24 kJ/mol. This means that the molecule has a hindered rotation for which an experimental barrier of 30 kJ/mol has been reported [34]. Note the local total energy minimum at a dihedral angle of 155° which is 1.4 kJ/mol lower in energy than the planar s-*cis*-form. Local minima in the region of 130° to 165° have been reported by several authors [35–37].

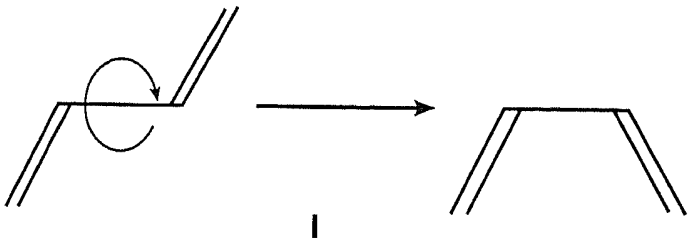

I

A more involved isomerization reaction is the transformation of norbornadiene (**N**) to quadricyclane (**Q**) **II** in which new bonds are formed. This reaction is a model case for photoconversion of solar energy into chemical energy and has, therefore, been discussed

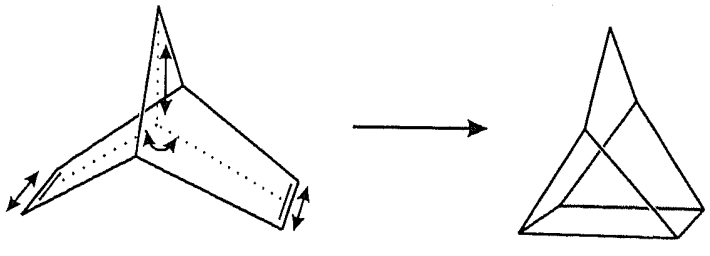

N **Q**

II

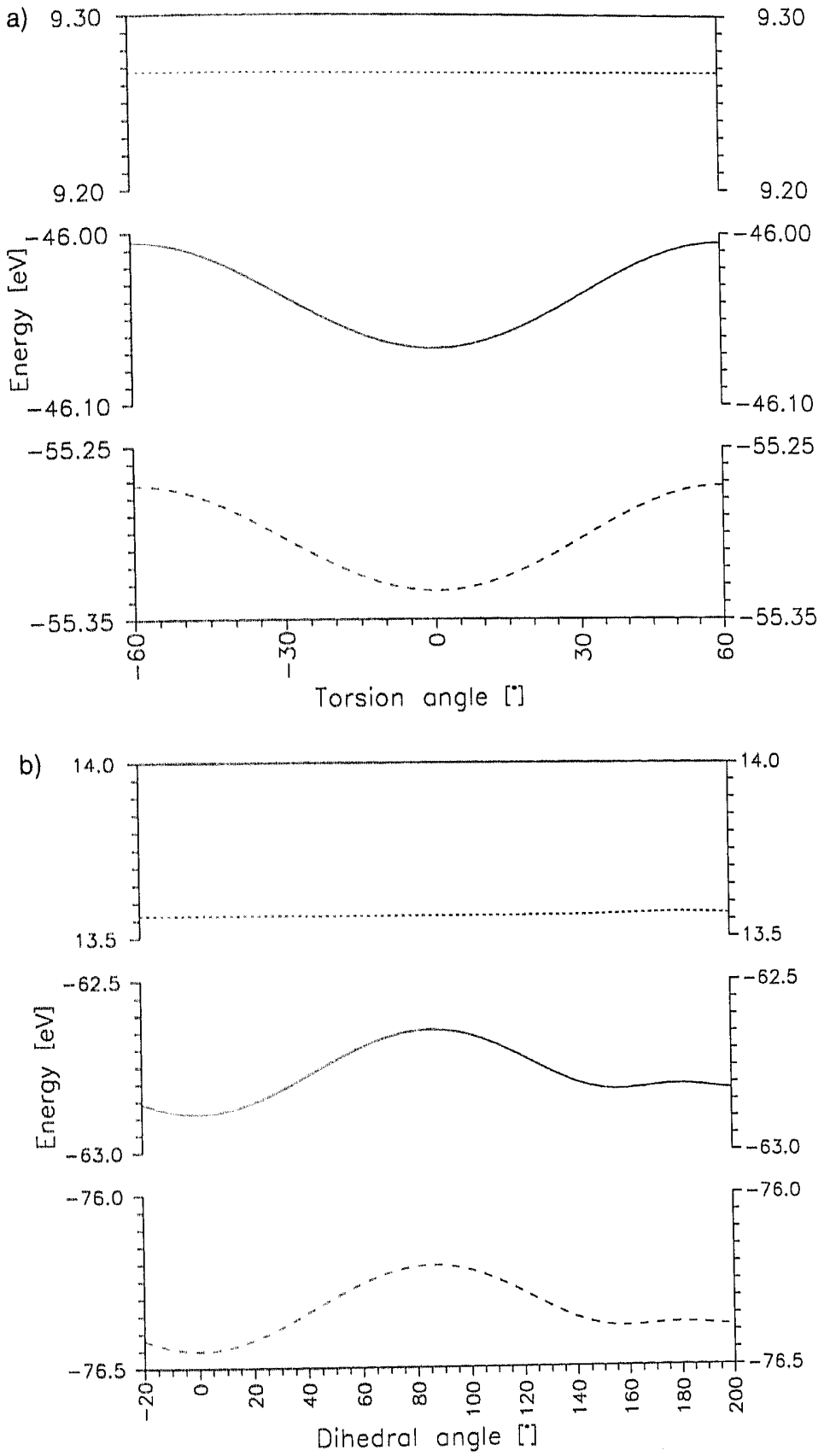

Fig. 3. *Energy as a function of the* a) *Me-group torsion in ethane and* b) *of the adiabatic s-*trans/*s-*cis-*isomerization of buta-1,3-diene* **I**. In *a*) 0° corresponds to the staggered conformation, while −60° and 60°, respectively, correspond to the eclipsed conformation. In *b*) 0° corresponds the s-*trans*-conformation and 180° corresponds to the s-*cis*-conformation. (----): Two-body interaction E_{Rep}, (——): total energy $E_{tot} = \Delta E_{EHMO} + E_{Rep}$, (- - - -): extended-*Hückel* binding energy ΔE_{EHMO}.

extensively [38] [39]. The correspondence of our calculated equilibrium geometry for norbornadiene and for quadricyclane with the experimental data is consistent with the results given in *Table 2*. In case of norbornadiene, we find a C=C distance of 1.30 Å and a dihedral angle of 112° which compares well with the experimental values of 1.343 Å and 115.6°, respectively. For **Q**, we find r(C–C) = 1.60 Å (experimental 1.53 Å) and a dihedral angle of 70° (experimental 63°). What is the influence of $E_{Rep}(R)$ along the chosen reaction path **II**? To find the answer, we have varied the angle between the planes of the C=C bonds and the C,C distance together with the height of the bridge independently. The resulting energy surface E_{tot} for r(C–C) *vs.* the angle between the planes and the C,C distance is shown in *Fig. 4*. We note that ΔE_{EHMO} does not show a minimum in the region of the norbornadiene, while there is one at the quadricyclane geometry. Addition of the electrostatic two-body repulsion E_{Rep} to ΔE_{EHMO} repairs this deficiency, as illustrated in *Fig. 4*. Similar situations are found in many of the following examples, a fact that will not be mentioned further. The calculated activation energy of 100 kJ/mol for the **Q** → **N** reaction seems reasonable and, as in the experiment, **N** turns out to be more stable than **Q**. However, the calculated reaction enthalpy ΔH_r, (**N** → **Q**) = 449 kJ/mol is much too large with respect to the experimental value of 112 kJ/mol. We shall come back to this later.

In the **N** → **Q** transformation, we have studied a case with ring strain in which two C=C bonds are transformed into four C–C bonds. What happens if two C=C bonds plus a C≡C bond are reacted to form five C–C bonds and one C=C bond? A reaction in which this takes place is the [2 + 2 + 2] cycloaddition of ethine to norbornadiene **III** in which deltacyclene is formed. Exothermic room-temperature Co-triphenylphosphine-Zn catal-

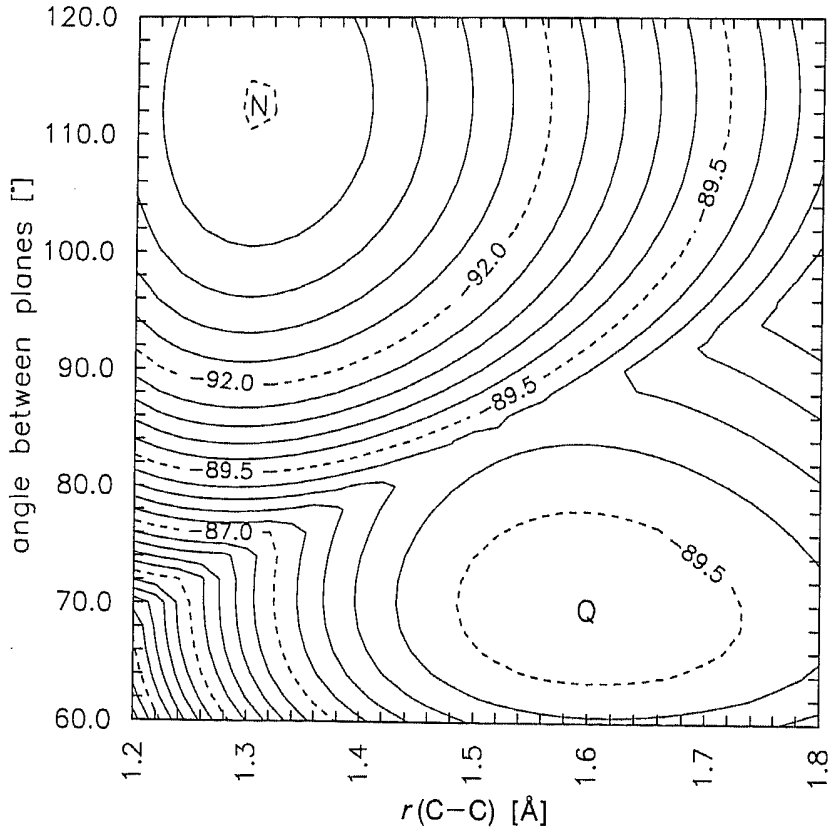

Fig. 4. *Potential-energy surface* E_{tot} [eV] *of the norbornadiene* (**N**) *to quadricyclane* (**Q**) *isomerization* **II**

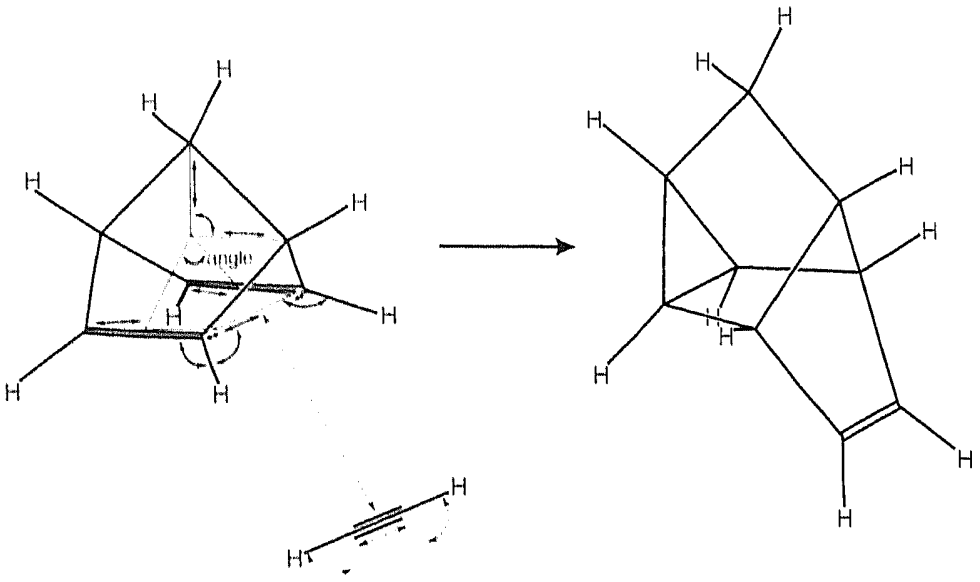

1 2

III

ysis of this homo-*Diels-Alder* reaction has been reported recently [40]. One expects that the reaction should be enthalpy-driven by about $\Delta H = -162$ kJ/mol, based on an estimation of the heats and entropies of formation from group contributions including ring strains after *Benson* [41]. Let us see whether we are able to describe the geometry of the product molecule deltacyclene. We chose a mixture of quadricyclane and norbornadiene coordinates as starting point of the geometry-search procedure. From this, we proceeded along the internal coordinates illustrated in **III(1)**. The finally obtained bond lengths and angles given in **IV** look reasonable and they are consistent with the results in *Table 2*.

Analysis of the frontier orbitals of **III(1)** shows an interaction between the HOMO of ethine and the LUMO of norbornadiene. From the argument of optimum overlap and also from a potential surface calculation, it can be shown that ethine approaches norbornadiene as indicated in **III(1)**. The plane defined by the dashed line and the ethine forms

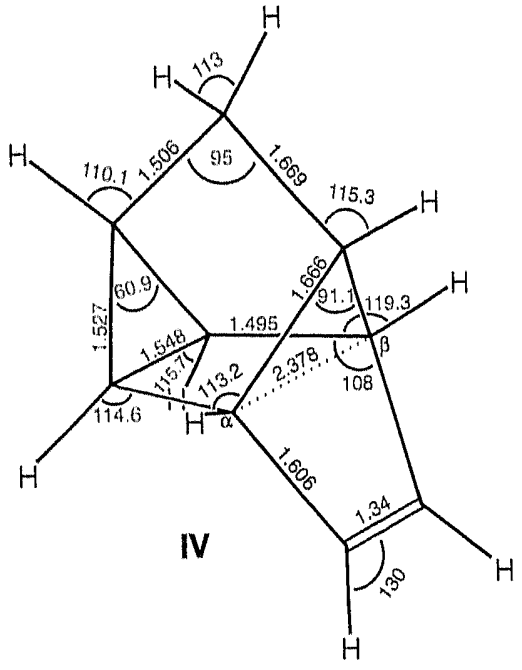

IV

an angle of 116° with the plane of the four double-bonded C-atoms in the norbornadiene. Investigation of the motions of the H-atoms connected to C_α and C_β and of the angle between the norbornadiene planes, as in **II**, led to the chosen reaction path **III**. To visualize it, this multidimensional reaction coordinate has to be simplified to its main features. A good possibility is to couple the motions indicated by the same type of lines in **III(1)**. This leads to the two-dimensional energy potential surface in *Fig. 5* in which **1** corresponds to only slightly disturbed separated norbornadiene plus ethine, at an angle of

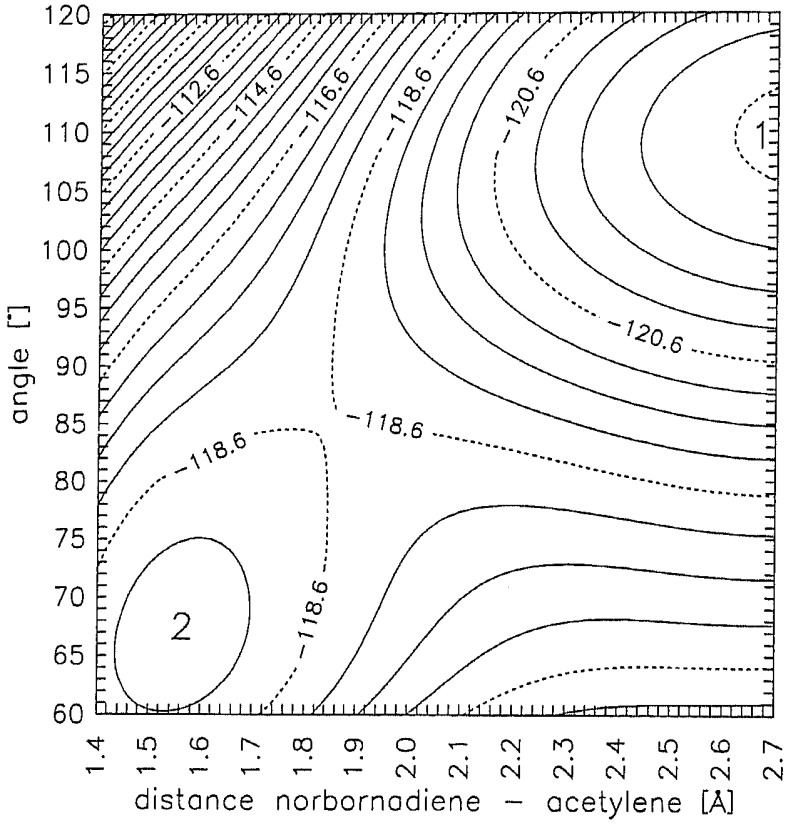

Fig. 5. *Potential-energy surface* E_{tot} [eV] *of the reaction path* **III**, *namely the addition of ethine to norbornadiene* (**1**) *to form deltacyclene* (**2**)

110°. Formula **2** represents the deltacyclene with an angle of 67° and an ethine-to-norbornadiene distance of 1.56 Å. All this looks reasonable. However, the reaction is predicted to be endergonic by 324 kJ/mol. Thus, we face the problem already encountered in the **N→Q** case in a more pronounced form. While the geometry turns out to be good, and while the general shape of the potential-energy surfaces makes sense, the reaction enthalpy calculated for the transformation of C≡C bonds to C=C bonds, and C=C bonds to C–C bonds is wrong. A similar situation is encountered in the next example where we analyze the decay of benzene to three ethine molecules along the reaction path **V** in which alternate C–C bonds have been simultaneously elongated in 0.10 Å steps and shortened in 0.01 Å steps. The C–C–H angles have been varied in 5° steps from 60° to 0°, independent of C–C stretching modes. The final distance of the three ethines from their centre of gravity is *ca.* 3.8 Å. The C–H bond lengths have been kept fixed. In the resulting potential-energy surface not shown, we observe two minima separated by a large barrier, one representing the three ethine molecules and the other one representing the benzene.

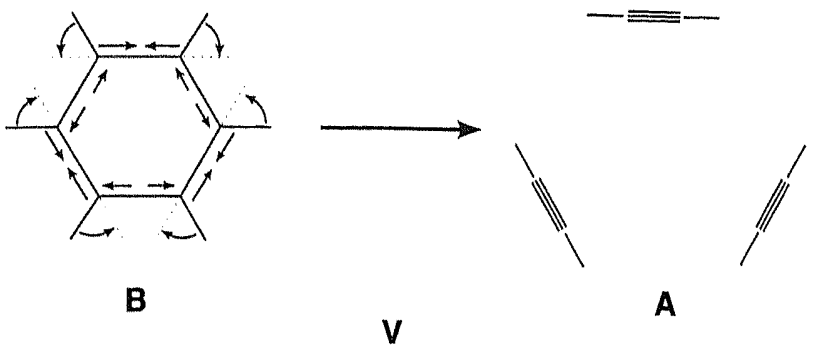

This and the calculated bond lengths reported in *Table 2* are correct. But the total energy of the three ethine molecules with respect to the benzene is largely overestimated. To summarize, we observe that the energy of C≡C bonds is overestimated with respect to C=C bonds, and that the energy of C–C bonds is underestimated with respect to C=C bonds.

Remember the general trend in *Table 2*. The calculated C–C bonds are too large, the C=C bonds are nearly precise, and the C≡C bonds are a bit too short. We know that bond lengths and dissociation energies do depend on the parameters κ and δ of *Eqn. 5* [21]. What is the influence of κ, which determines K at $R = d_0$, on the calculated C,C bond lengths of ethane, ethene, and ethine as simplest representatives of C–C, C=C, and C≡C bond hydrocarbons? To answer this, we have optimized the geometry of these molecules at κ values ranging from 0.85 to 1.25. The result of this calculation is illustrated in *Fig. 6*.

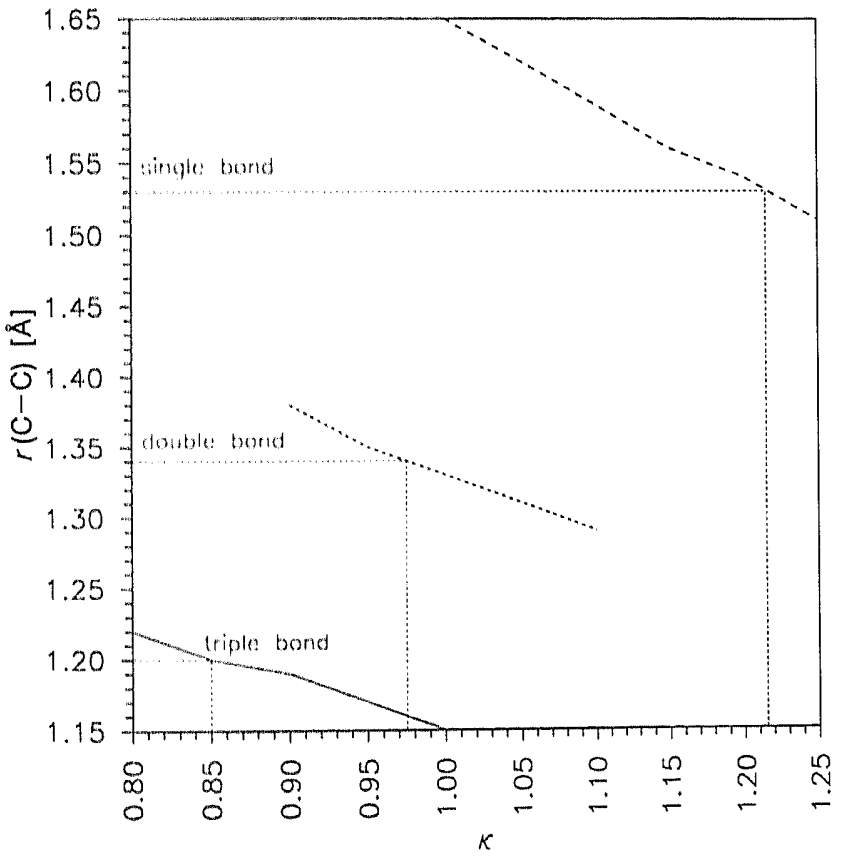

Fig. 6. *C–C Bond length r (C–C) as a function of κ for C–C, C=C, and C≡C bonds.* Experimental bond lengths of ethane, ethene, and ethine, and the corresponding κ values are marked by dashed lines.

In each case, it indicates a nearly linear dependence of the bond length on κ, which is physically reasonable. Connecting the experimental C,C distances from the left to right with a tolerance of *ca.* 0.01 Å by a straight line, we observe that the following relation holds:

$$\kappa = \kappa_0 + r\,(\mathrm{C,C}) - d_0 \tag{14}$$

The ζ_{2p} *Slater* exponent of carbon leads to $d_0 = 1.31$ Å [21] which is approximately equal to the C=C bond length. From this and from *Fig. 6* follows that $\kappa = 1.0$ is a good choice for describing the C=C bond. C≡C Bonds demand a κ of *ca.* 0.85, and for C–C bonds, it should be close to 1.2. We would like to emphasize that *Eqn. 14* has to be understood as a relation between sp, sp^2, and sp^3 C-atoms and has, therefore, to be applied accordingly. This means that *e.g.* in buta-1,3-diene $\kappa = 1.0$ can be applied, because all four C-atoms are sp^2, see *Table 2*. Remember that κ does not only influence bond lengths, but also the stabilization energy of a molecule, given by *Eqns. 3, 8,* and *9*. From the *Wolfsberg-Helmholz* approximation follows that the resonance energy H_{ij} decreases with decreasing K. A smaller K at equilibrium bond length causes a decrease of the absolute value of ΔE_{EHMO}. This means that increasing κ with increasing equilibrium bond length according to *Eqn. 14* should lead to more accurate energy behavior. This general idea can be tested by calculating the reaction enthalpy $\Delta H_r = E$ (cyclobutane)–E (2 · ethene) of the transformation of two ethene molecules to cyclobutane **VI**, by keeping parameters constant except κ (C–C) for the C–C bonds of cyclobutane. As before, we have optimized the geometry at each κ point. The enthalpy of formation decreases with increasing κ as expected. A nearly linear dependence is found which can be expressed as

$$\Delta H_r = \Delta H_{r,0} - a_h(\kappa - \kappa_0) \tag{15}$$

with $a_h = 33$ eV. The experimental reaction enthalpy is –0.81 eV [41] [42]. This enthalpy is obtained, if the calculation is carried out with κ (C–C) = 1.08 which leaves the r(C–C) distance too large by only 0.06 Å instead of 0.11 Å. By improving the reaction enthalpy we have also improved the bond length.

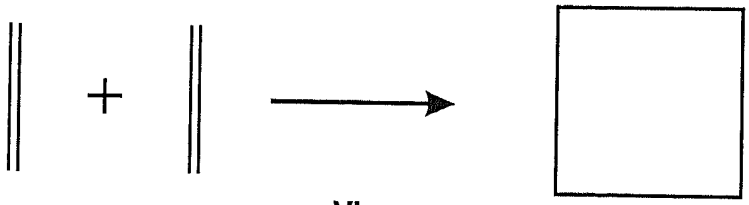

VI

Provided that our argument be correct, it must equally apply to the conversion of C≡C bonds to C=C bonds as *e.g.* in the case of the ethine-to-benzene transformation **V**. We have calculated the reaction enthalpy of the transformation of three ethine molecules into benzene, $\Delta H_r = E$ (benzene) – E (3-ethine), by keeping parameters constant, except κ for ethine. E (benzene) was calculated with $\kappa = 1.0$ and the C≡C and C–H bond lengths of ethine were optimized for each κ (C≡C). We observe the linear dependence (*Eqn. 15*) again, but now of course with negative a_h which is equal to –83 eV. The experimental reaction enthalpy of –6.2 eV [41] [42] is obtained with κ (C≡C) = 0.9. With this κ, the calculated bond length differs by only *ca.* 0.01 Å from the experimental value.

The third type of reaction to test is the conversion of C=C plus C≡C bonds to C–C and C=C bonds. This can be done by studying the 2 · ethene + ethine→cyclohexene transformation **VII** which has been calculated with κ (C–C) = 1.1, κ (C=C) = 1.0, and κ (C≡C) = 0.9. Reoptimization of the geometry of cyclohexene results in r(C=C) = 1.33 Å, in C–C bond lengths of the C-atoms adjacent to the C=C bond of r (C–C) = 1.53 Å and a mean value of $\bar{r}$ (C–C) = 1.58 Å for the other C–C bonds. These values compare well with the experimental data in *Table 2*. The calculated reaction enthalpy for **VII** amounts to ΔH_r = −471 kJ/mol. It is too large compared to ΔH_r(exp.) = −335 kJ/mol but has improved much with respect to calculations with a global κ of 1.0. The application of the same κ values to the six-ring formed by the previously discussed thermally allowed [2 + 2 + 2] addition **III** yields an estimate of the reaction enthalpy ΔH_r of −392 kJ/mol, which is reasonable. We conclude that the simple κ adjustment (*Eqn. 14*) opens a way to not only calculate bond geometries but also to estimate reaction enthalpies.

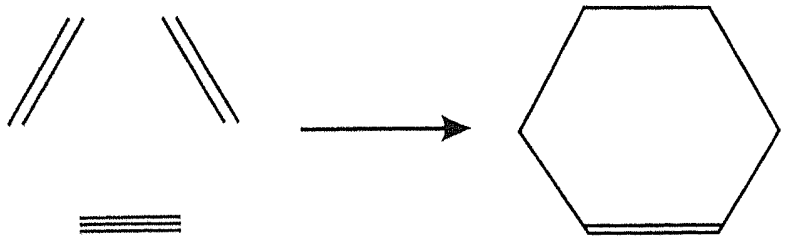

VII

What about enthalpies of formation ΔH_f? There is no need to calculate the absolute values of enthalpies of formation to describe reaction enthalpies, since the standard enthalpy of formation of a substance is the standard enthalpy for its formation from its elements in their reference states. It is, however, necessary that a linear relationship of the following type holds

$$\Delta H_{f,\text{exp.}} = \Delta H_{f,\text{calc.}} + \sum_{\alpha} \Delta_{\alpha} \tag{16}$$

where Δ_α is the deviation with respect to each atom α. In reaction enthalpies, deviations of the enthalpies of formation cancel, if this equation is fulfilled with constant $\Delta\alpha$ for any molecule. The cases to be investigated in this context are the C–C, the C=C, and the C≡C bond molecules ethane, ethene, and ethine for which experimental and calculated data are reported in the upper part of *Table 3* for κ = 1.0 and for the adapted κ. The experimental heats of formation in this table are given with respect to the atoms in the gas phase, to make them comparable with the calculated values. It is obvious that *Eqn. 16* is not fulfilled for κ = 1. For the κ values (1.215, 0.975, 0.85), however, the following equation holds

$$\Delta H_{f,\text{exp.}} = \Delta H_{f,\text{calc.}} - J_C \cdot 0.5\ \text{eV} - J_H \cdot 3.0\ \text{eV} \tag{17}$$

where J_C denotes the number of C-atoms and J_H the number of H-atoms in the molecule. This finding is consistent with our observation that reaction enthalpies ΔH_r of hydrocarbons can be estimated with optimized (δ,κ) parameters. Let us look at the energy partitioning *Eqns. 10–13*. According to *Eqns. 10–13*, $\Delta E_{\text{EHMO}_\alpha}$ is the binding energy gain of an atom in a molecule, E_{Rep_α} is the repulsion loss and E_α is the total energy gain.

Table 3. *Experimental and Calculated Heats of Formation and Their Splitting into Atom Contributions for Ethine, Ethene, and Ethane in Their Minimum Geometry.* All values in [eV].

	$\Delta H_{f,\text{exp.}}$	Diff.	$\Delta H_{f,\text{calc.}}(\kappa)$	Diff.	$\Delta H_{f,\text{calc.}}(\kappa)$	Diff.
C_2H_6	29.29		46.01 (1.0)		47.84 (1.215)	
C_2H_4	23.35	5.94	36.39 (1.0)	9.62	35.94 (0.975)	11.90
C_2H_2	17.03	6.32	27.78 (1.0)	8.61	23.52 (0.85)	12.42
κ		E_{EHMO_α}	$\sum_s b_s^0 E_s^0$	$\Delta E_{\text{EHMO}_\alpha}$	E_{Rep_α}	E_α
Atomic contributions						
1.0	C_2H_2					
	H	–18.4104	–13.6	–4.8104	0.8606	–3.9498
	C	–78.9466	–65.6	–13.3466	3.4014	–9.9452
1.0	C_2H_4					
	H	–18.5164	–13.6	–4.9164	0.7414	–4.1750
	C	–77.9079	–65.6	–12.3079	2.4652	–9.8427
1.0	C_2H_6					
	H	–18.5755	–13.6	–4.9755	0.7446	–4.2309
	C	–78.3207	–65.6	–12.7207	2.3994	–10.3213
0.85	C_2H_2					
	H	–18.7399	–13.6	–5.1399	0.9058	–4.2341
	C	–75.9894	–65.6	–10.3894	2.8629	–7.5265
0.975	C_2H_4					
	H	–18.5671	–13.6	–4.9671	0.7411	–4.2260
	C	–77.5322	–65.6	–11.9322	2.4140	–9.5182
1.215	C_2H_6					
	H	–18.2828	–13.6	–4.6828	0.7082	–3.9746
	C	–80.0270	–65.6	–14.4270	2.4437	–11.9833

Remember that for $\kappa = 1.0$, the stabilization of ethine is overestimated. This can be understood, when we judge the results of the detailed analysis in the second part of *Table 3*. We see that for a constant $\kappa = 1$, the stabilization ΔE_{EHMO_C} of a C-atom in ethine is too large with respect to the stabilization in ethene and ethane. The adapted κ values, however, lead to the correct trend.

4. Water and Organic Molecules Containing Oxygen, Sulfur, and Nitrogen. – In one of his early papers, *Hoffmann* mentions that the simplified *Slater* parameters in *Table 4* tend to a wide bond angle for the H_2O molecule, and that this can be influenced by the 1s orbitals of hydrogen [2c]. Later, it was stated that EHMO calculations predict linear water geometry [43], but calculation with the simplified *Slater* parameters results in a

Table 4. Slater *Parameters for C,N,O,S*

Element	Simplified [2]		*Slater* rule [15]		This work	
	2s	2p	2s	2p	2s	2p
C	1.625	1.625	1.95	1.625	1.71	1.625
N	1.95	1.95	2.475	1.95	2.14	1.95
O	2.275	2.275	2.975	2.275	2.575	2.275
S	2.122	1.827	2.283	1.817	2.283	1.817

H–O–H angle of 157° at an O–H bond length of 0.96 Å. This result is not markedly influenced by the electrostatic two-body correction. The calculated H–O–H angle is, however, sensitive to the 2s *Slater* parameter of oxygen. An angle of 133° is calculated, if for example $\zeta_{2s} = 2.575$ is chosen while keeping ζ_{2p} at its original value of 2.275. Let us look at the *Walsh* diagram in *Fig. 7* to understand how this occurs. It illustrates the energies of the occupied levels of H_2O for the two ζ_{2s} values 2.275 and 2.575. The only orbital that changes its energy behavior along the bending angle with changing ζ_{2s} is the HOMO + 1 which can be expressed as:

$$\Phi_{\text{HOMO}+1} = C_{1s} \cdot (1s_1 + 1s_2) - C_{2s} \cdot 2s + C_{2p_z} \cdot 2p_z \tag{18}$$

This means that the influence of ζ_{2s} on the calculated angle is only determined by the changing slope of the HOMO + 1 level. The reason for this is the negative 2s-oxygen contribution to this orbital. Contraction of the 2s AO causes a smaller $< 1s|2s >$ overlap, *e.g.* 0.41 for $\zeta_{2s} = 2.575$ instead of 0.46 for $\zeta_{2s} = 2.275$ at r (O–H) = 0.96 Å, and, therefore, a smaller 2s contribution to the energy of the HOMO + 1. The $< 1s|2s >$ overlap does not depend on the angle while $< 1s|2p_z >$ increases with decreasing angle thus causing a more rapid stabilization of the HOMO + 1 level for the more contracted 2s AO. The decrease of the $< 1s|2s >$ overlap with increasing ζ_{2s} is responsible for the destabilization of the HOMO + 3 and causes a small increase of the bond length.

Having a qualitative understanding of the influence of ζ_{2s} on the bond angle, we would like to know quantitatively how the O–H bond length and the H–O–H angle are related to the oxygen *Slater* parameters. To get this information, we have to calculate the bond

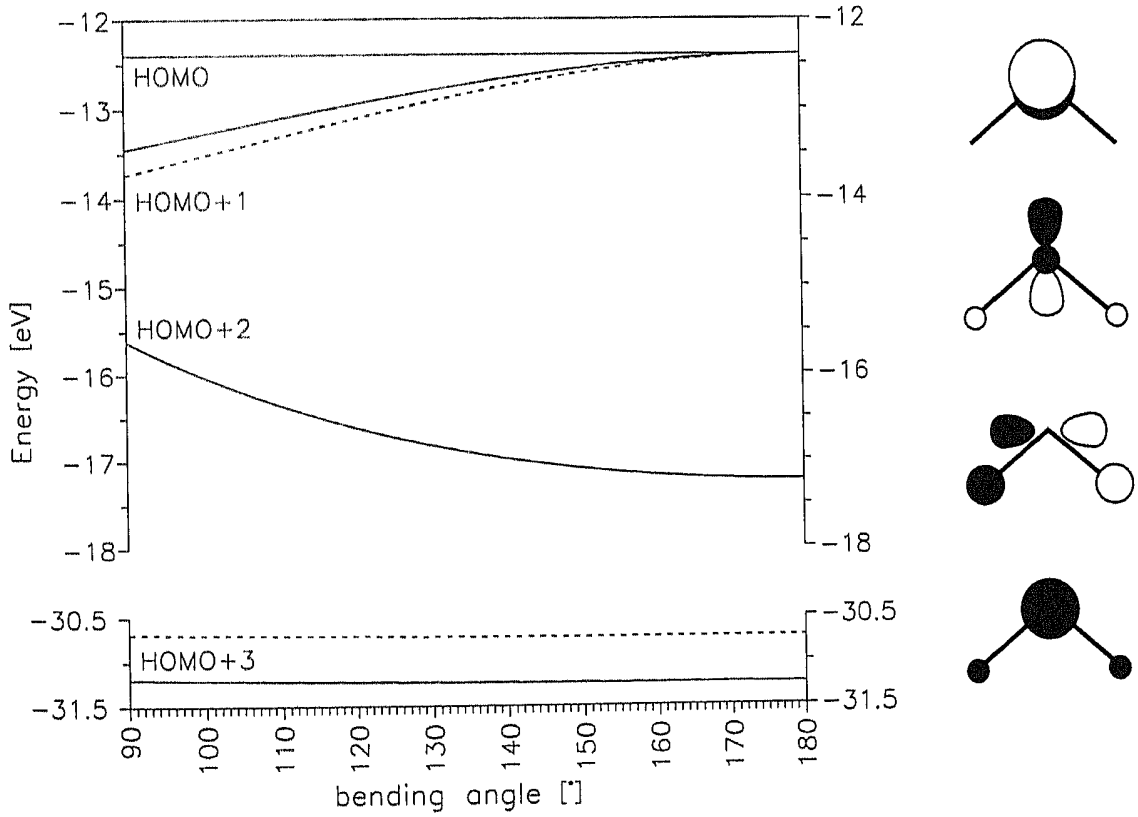

Fig. 7. Walsh *diagram of the occupied orbitals of* H_2O *for two different* ζ_{2s} *values, while* ζ_{2p} *was kept at 2.275.* (——): $\zeta_{2s} = 2.275$, (· · ·): $\zeta_{2s} = 2.575$.

length and the bond angle by varying ζ_{2s} and ζ_{2p} independently. We are further interested in the effect of charge iteration on the results and have, therefore, chosen the following procedure: charge iteration on O and H was carried out at the experimental equilibrium geometry to get optimized *Coulomb* integrals for each (ζ_{2s}, ζ_{2p}) set. O–H Distances and bond angles have been varied at intervals of 0.01 Å and 1.0°, respectively. Each potential surface generated was searched for its energy minimum which served as a point in *Fig. 8a, b*, where the calculated equilibrium O–H bond lengths and H–O–H bond angles are plotted as a function of the oxygen *Slater* parameters. We already know that the H–O–H angle decreases with increasing ζ_{2s}. New in *Fig. 8a* is that the angle increases with

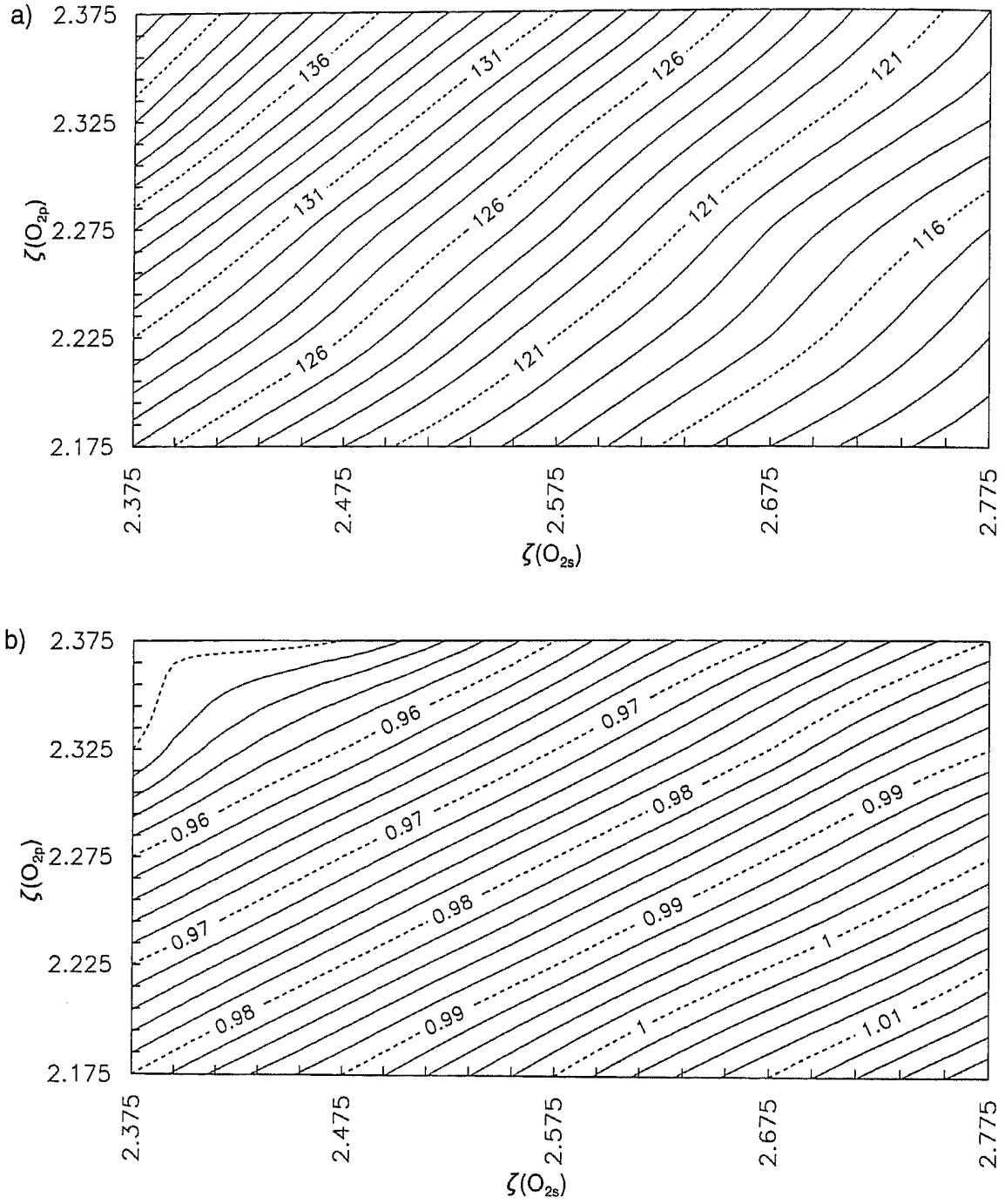

Fig. 8. *Minimum geometry as a function of the oxygen* Slater *parameters* (ζ_{2s}, ζ_{2p}). *a*) H–O–H angle [°], *b*) O–H distance [Å].

increasing ζ_{2p}. If ζ_{2p} is sufficiently small and ζ_{2s} sufficiently large, the experimental bond angle can be reproduced. But we already know that not only the bond angle but also the bond length is influenced by the *Slater* parameters. This is illustrated in *Fig. 8b*. Fortunately, both figures show simple behavior. An acceptable compromise to get good bond lengths with a reasonable bond angle is, therefore, possible without the need of adjusting κ and/or δ. $\zeta_{2s} = 2.575$ and $\zeta_{2p} = 2.275$ is adequate for our purposes.

Using contracted ζ_{2s} *Slater* parameters is not a disadvantage. The simplified 2s *Slater* parameters do not reflect the contraction of the 2s valence shell with respect to 2p caused by the stronger charge attraction of the higher charged cores of the more electronegative atoms on the right side of the periodic table. From *Fig. 8a,b* follows, however, that if we contract as much as demanded by the *Slater* rule [15], we move into a region where unpredictable behavior can not be excluded. To get a consistent set of 2s *Slater* parameters for the other elements discussed in this paper, we have scaled the *Slater* parameters ζ_{2s} by the factor 2.575/2.975 = 0.866. The so obtained values for C,N,O are collected in the right column of *Table 4* and correspond to those of *Table 1*. 2s *Slater* parameters for the other 2nd period elements can be estimated by similar arguments. Note that the 2s value of carbon differs little from the simplified set, and that this difference has only minor influence on the results.

By choosing the H_2O molecule to discuss the influence of the oxygen *Slater* parameter on the geometry, we hoped that the results would be significant for O-containing organic molecules. The first two representative molecules to be tested were CH_3OH and $CH_3{-}O{-}CH_3$. The results in *Table 5* show that $\zeta_{2s} = 2.575$ works well for the bond angles

Table 5. *Experimental and Calculated Angles* [°] *and Bond Lengths* [Å] *of Water, Methanol, Dimethyl Ether, Ethylene Oxide, and Their Sulfur Analogues*

Molecule	r(O–C)		r(O–H)		r(C–H)		α(R^1–O–R^2)		α(O–C–H)	
	Exper.	Calc.	Exper.	Calc.	Exper.	Calc.	Exper.	Calc.	Exper.	Calc.
H_2O			0.958	0.97			104.6	133		
CH_3OH	1.425	1.55	0.954	0.94	1.094	1.07	108.5	132.5	110.3	102
CH_3OCH_3	1.41	1.49			1.09	1.10	117	126	109.5[a])	104
Molecule	r(S–C)		r(S–H)		r(C–H)		α(R^1–S–R^2)		α(S–C–H)	
	Exper.	Calc.	Exper.	Calc.	Exper.	Calc.	Exper.	Calc.	Exper.	Calc.
H_2S			1.336	1.23			92.1	104		
CH_3SH	1.814	1.82	1.335	1.22	1.092	1.08	96.5	101	109.8	110
CH_3SCH_3	1.802	1.82			1.091	1.08	98.9	101	109.5[b])	110
Molecule[d])	r(C–C)		r(C–X)		Θ_2[c])					
	Exper.	Calc.	Exper.	Calc.	Exper.	Calc.				
$(CH_2)_2O$	1.48	1.54	1.43	1.43	158	164				
$(CH_2)_2S$	1.49	1.60	1.81	1.80	152	143				

[a]) Mean value of all angles.
[b]) Mean value of all angles.
[c]) Angle between the C–C bond and the intersect of H–C–H.
[d]) Calculations have been carried out at fixed experimental values for the H–C–H angle and the C–H bond length. For a discussion see *Sect. 5*.

α (R^1–O–R^2) and α (O–C–H), and that also the calculated bond lengths are reasonable. The tendency of O–C bond lengths to be too large by *ca.* 0.08 Å and 0.125 Å can be discussed as in case of the C–C bond length of hydrocarbons. We skip this since the arguments are the same. Our procedure is not restricted to first- and second-period elements. This has already been demonstrated for Si [22] and some other elements [23]. We add the three representative organic sulfur compounds in *Table 5*. The calculated bond lengths and bond angles are consistent with the experimental values.

The three exemplary C=O bond molecules are formaldehyde, methaldehyde, and acetone. The calculated and the experimental bond lengths and angles of these molecules in *Table 6* show that the calculated r (C=O) are too large by 0.04–0.07 Å, but the shortening tendency when going from single to double is well represented, and the angles come out well.

The carbonic acids seem to be more critical. If the geometry is optimized at the experimental α (C–O–H) angle, the distance r (C=O) comes out shorter than r (C–OH), as it should be. While the O–C=O and the H–C=O angles agree well with the experiment, α (C–O–H) comes out much too large. As a consequence, the optimized bond distances at this angle are wrong, because the energy minimum is determined by the repulsion. This problem can be avoided by optimizing parameters as mentioned above.

The comparison of calculated and experimental data in *Table 7* of exemplary N-containing organic molecules shows that the bond lengths come out well. Also the bond angles of most molecules are satisfactory. In the case of the three-ring ethyleneimine, charge iteration at the experimental geometry was applied to get a consistent set of *Coulomb* integrals, see *Table 7*. This leads to an improvement of the calculated angle Θ_1 as defined in **IX** from 160° to 130°. The angle between the C–N bond and the intersect of the H–N–H angle of methylamine form a pyramidal structure which looks reasonable. We already know that ammonia comes out flat [2]. Polarization functions must be included to describe the tunnelling barrier of this molecule, *e.g.* in a second-order perturbation calculation [45] [46]. The same is true for aniline where we find that E_{tot} between a C–N–H_2 angle of 0 and $\pm$ 20° changes by less than 0.1 eV. The 'ammonia inversion' in this molecule is known to occur with a lifetime of $6.7 \cdot 10^{-12}$ s in dioxane and in benzene at room temperature [47], which means that the tunnelling barrier is low.

5. Three-Membered Rings. – Three-membered rings have attracted much interest, and stimulating theoretical studies based on the EHMO approach and also on more sophisticated theories have been carried out [48]. They are characterized by a set of valence orbitals, the *Walsh* orbitals, which confer unusual conformationally specific conjugative properties on these systems. Consequences of the presence of these orbitals on equilibrium geometries, spectra and reactivity have been discussed [6] [8] and the question, do *Walsh* orbitals exist, has been debated [49]. We have already seen in *Table 2* that the geometry of cyclopropane comes out well. The same is true for the potential energy along mode **VIII** in *Fig. 9a*. The analysis of E_{tot} and ΔE_{EHMO} shows that E_{Rep} is necessary to obtain such good results. If a CH_2 group is substituted by an NH, the r (–..X) mode becomes softer which is reasonable. The calculated bond lengths and angles are in good agreement with the experimental values given in *Table 7*. Note that the calculated ammonia angle Θ_1 defined in **IX** is accurate. The next logical step would be to replace NH by an O-atom. However, the epoxide molecule demands a more detailed discussion. Let us, therefore, first switch to the ethylene sulfide that plays a role in hydrodesulfurization

Table 6. *Experimental and Calculated Bond Lengths* [Å] *and Angles* [°] *of Carbonyl Compounds*

Molecule	$r(C^1{=}O)$		$r(C^1{-}C^2)$		$r(C^1{-}H)$		$r(C^2{-}H)$		$\alpha(R^1{-}C^1{-}R^2)$		$\alpha(R^1{-}C^1{=}O)$		$\alpha(H{-}C^2{-}H)$	
	Exper.	Calc.	Exper.	Calc.	Exper.	Calc.	Exper.	Calc.	Exper.	Calc.	Exper.	Calc.	Exper.	Calc.
HCHO	1.208	1.28			1.116	1.06			116.5	126	121.8	117		
CH_3CHO	1.216	1.26	1.501	1.55	1.114	1.05	1.086	1.08	117.5	123	123.9	120	108.3	109.9
CH_3COCH_3	1.222	1.27	1.507	1.54			1.085	1.08	117.2	124	121.4	118	108.8	109.9
Molecule	$r(C{=}O)$		$r(C{-}OH)$		$r(C{-}H)$		$r(O{-}H)$		$\alpha(O{-}C{=}O)$		$\alpha(H{-}C{=}O)$		$\alpha(C{-}O{-}H)$	
	Exper.	Calc.	Exper.	Calc.	Exper.	Calc.	Exper.	Calc.	Exper.	Calc.	Exper.	Calc.	Exper.	Calc.
HCOOH	1.202	1.36 1.25[a])	1.343	1.29 1.44[a])	1.097	1.03	0.972	0.97	124.9	115	124.1	122	106.3	143
Molecule	$r(C{=}O)$		$r(C{-}OH)$		$r(C{-}C)$		$r(O{-}H)$		$\alpha(O{-}C{=}O)$		$\alpha(C{-}C{=}O)$		$\alpha(C{-}O{-}H)$	
	Exper.	Calc.	Exper.	Calc.	Exper.	Calc.	Exper.	Calc.	Exper.	Calc.	Exper.	Calc.	Exper.	Calc.
CH_3COOH	1.212	1.35 1.24[a])	1.369	1.29 1.47[a])	1.517	1.50	0.972[b])	0.97	122.8	114	126.6	123	106.3[b])	143

[a]) Determined at fixed experimental bond lengths and angles (see text for explanation).
[b]) Assumed from formic acid.

Table 7. *Experimental and Calculated Angles* [°] *and Bond Lengths* [Å] *of Organic Compounds Containing Nitrogen*

Molecule	r(N–H)		r(C–N)		r(C–H)		α(N–C–H)		α(H–N–H)		Θ[a])	
	Exper.	Calc.	Exper.	Calc.	Exper.	Calc.	Exper.	Calc.	Exper.	Calc.	Exper.	Calc.
CH_3NH_2	1.010	1.00	1.471	1.56	1.099	1.07	110	106	107	108	–	52.5
Aniline[b])	0.998	0.99	1.431	1.53					114	122	39	0

Molecule	r(C–C)		r(C–N)		r(C–H)		α(H–C–C)	
	Exper.	Calc.	Exper.	Calc.	Exper.	Calc.	Exper.	Calc.
HCN			1.153	1.12	1.065	1.03		
CH_3CN	1.458	1.50	1.157	1.12	1.104	1.08	109.5	110

Molecule	r(N–N)		r(C–N)		r(C–H)		α(H–C–N)		α(C–N–N)	
	Exper.	Calc.	Exper.	Calc.	Exper.	Calc.	Exper.	Calc.	Exper.	Calc.
CH_3–N=N–CH_3	1.247	1.26	1.482	1.50	1.105	1.07	107.5	107	112	122

Molecule	r(C–C)		r(C–N)		r(N–H)		Θ_1[c])		Θ_2[d])	
	Exper.	Calc.	Exper.	Calc.	Exper.	Calc.	Exper.	Calc.	Exper.	Calc.
Ethylenimine[e])	1.481	1.56	1.475	1.52	1.016	0.99	67.5	50	155	157

[a]) Angle between C–N bond and intersect of H–N–H angle.

[b]) Fixed experimental geometry of Ph ring has been used.

[c]) As defined in **IX**.

[d]) Angle between C–C bond and the intersect of H–C–H. Calculation at fixed experimental values for the H–C–H angle and the C–H bond length.

[e]) Calculated with charge iterated *Coulomb* integrals H_{ii}/eV: N: $H_{2s2s} = -22.76$; $H_{2p2p} = -10.89$; C: $H_{2s2s} = -20.37$; $H_{2p2p} = -11.44$; H_N: $H_{1s1s} = -14.23$, H_C: $H_{1s1s} = -13.60$.

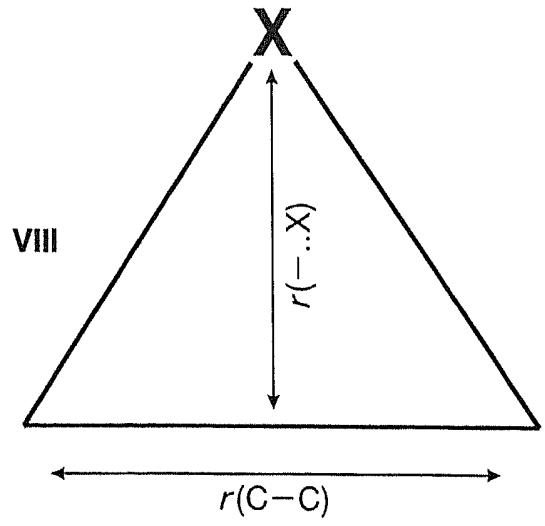

VIII

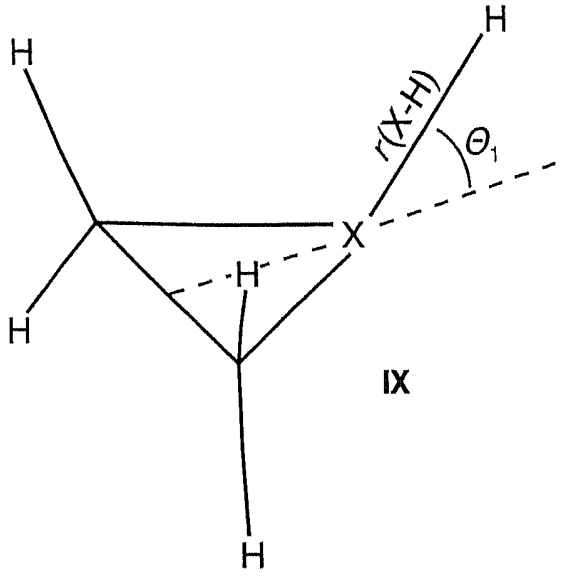

IX

on molybdenium-sulfide catalyst which has been investigated recently [50]. We do not show the potential-energy surface, because it looks similar to that in *Fig. 9b*. The calculated C–S distance is close to the observed value of 1.815 Å. As expected from the discussion in the hydrocarbon section r (C–C) = 1.6 Å is too long, it should be 1.484 Å, while r (C–H) = 1.06 Å is close to the experimental value of 1.08 Å and the C–CH_2 'wagging angle' of 143°, defined in the same way as Θ_2 of ethylenimine compares well to the experimental value of 152°.

If ethylene oxide is calculated with the $(\kappa, \delta) = (1.0, 0.35\ \text{Å}^{-1})$ values, used for most calculations in this paper, the r (—..O) distance comes out too long by 0.5 Å with a very shallow potential along the r (—..X) coordinate **VIII**. From discussing the hydrocarbons (*Fig. 6*), we already know that an increase of κ (C–O) should lead to a shorter and hence more realistic bond length. We have, therefore, investigated the influence of κ (C–O) on r (C–O) by keeping the other parameters constant. This is illustrated in *Fig. 10*. It shows the dependence of r (—..O) and r (C–C) on κ (C–O). κ (C–O) has a relatively small effect on r (C–C), as expected. The experimental C–O bond length of 1.43 Å which corresponds to r (—..O) = 1.20 Å is reproduced at κ (C–O) = 1.2. At this value, the C–C bond length of 1.55 Å is too long by *ca.* 0.07 Å. The C–CH_2 'wagging angle' of 164° compares

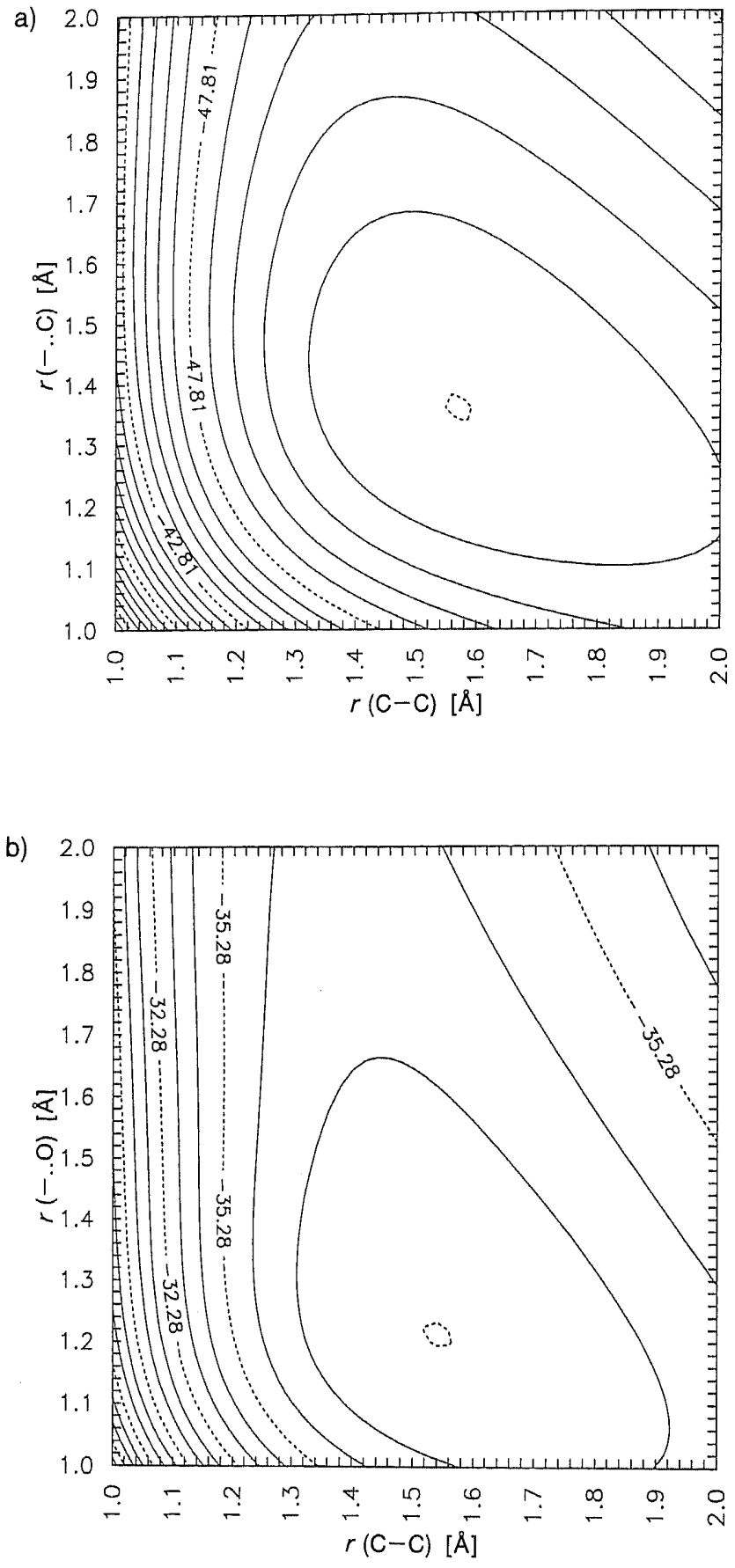

Fig. 9. *Potential-energy surfaces* E_{tot} [eV] *of the motion* **VIII** *of three-membered rings. a)* r (–.. C): Cyclopropane. *b)* r (–.. O): Ethylene oxide (κ (C–O) = 1.2).

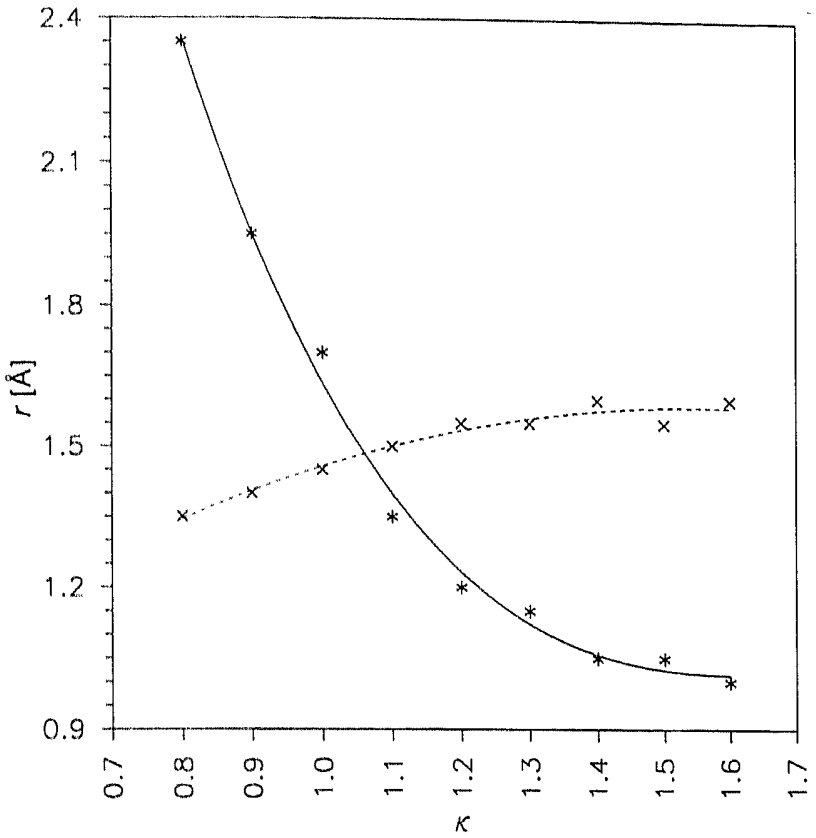

Fig. 10. *r(–..O) distance* (——) *and C'–C' bond length* (----) *of ethylene oxide as function of* κ*(C–O)*. The calculated points are interpolated by a quadratic polynomial. r(–..O) = 1.2 Å corresponds to the experimental bond length r(C–O) = 1.43 Å.

well with the experimental value of 158° and the resulting potential-energy map in *Fig. 9b* appears to be reasonable. This means that κ(C–O) = 1.2 solves the ethylene-oxide problem. To understand why this is so, we compare the r(–..O) mode **VIII** for κ(C–O) = 1.0 and κ(C–O) = 1.2. Calculations have been carried out at the corresponding C–C bond length of 1.42 Å and 1.54 Å, respectively. The resulting two-body repulsion, the stabilization and the total energy are shown in *Fig. 11a*. The difference between the repulsion-energy curves in the left region is caused by the different C–C distances used in the two calculations since E_{Rep} is independent of κ. The geometry depends mainly on the ΔE_{EHMO} curve which decreases much faster for κ(C–O) = 1.2 than for κ(C–O) = 1.0. This explains why optimization of κ works. It would be interesting to know which orbitals are responsible for this ΔE_{EHMO} dependence on κ(C–O). This question is readily answered by looking at the correlation diagram in *Fig. 11b*. The b_1 orbital denoted as HOMO + 1 is the only bonding orbital which changes its shape in the binding region in a favorable way when going from κ(C–O) = 1.0 to 1.2. In addition, the more pronounced bonding interaction of the HOMO + 2 at long r(–..O) helps to obtain a realistic potential energy curve. This orbital becomes strongly antibonding at short bond lengths. The sum of the favorable and unfavorable contributions of the less important lower-lying orbitals not shown here results in a net gain of ΔE_{EHMO}.

Considering the antibonding character of the HOMO + 2 at short r(–..O), one expects that withdrawal of electron density from this orbital should increase the stability of the r(C–O) bond. Withdrawal of electron density can be achieved by addition of polarization functions of the right symmetry.

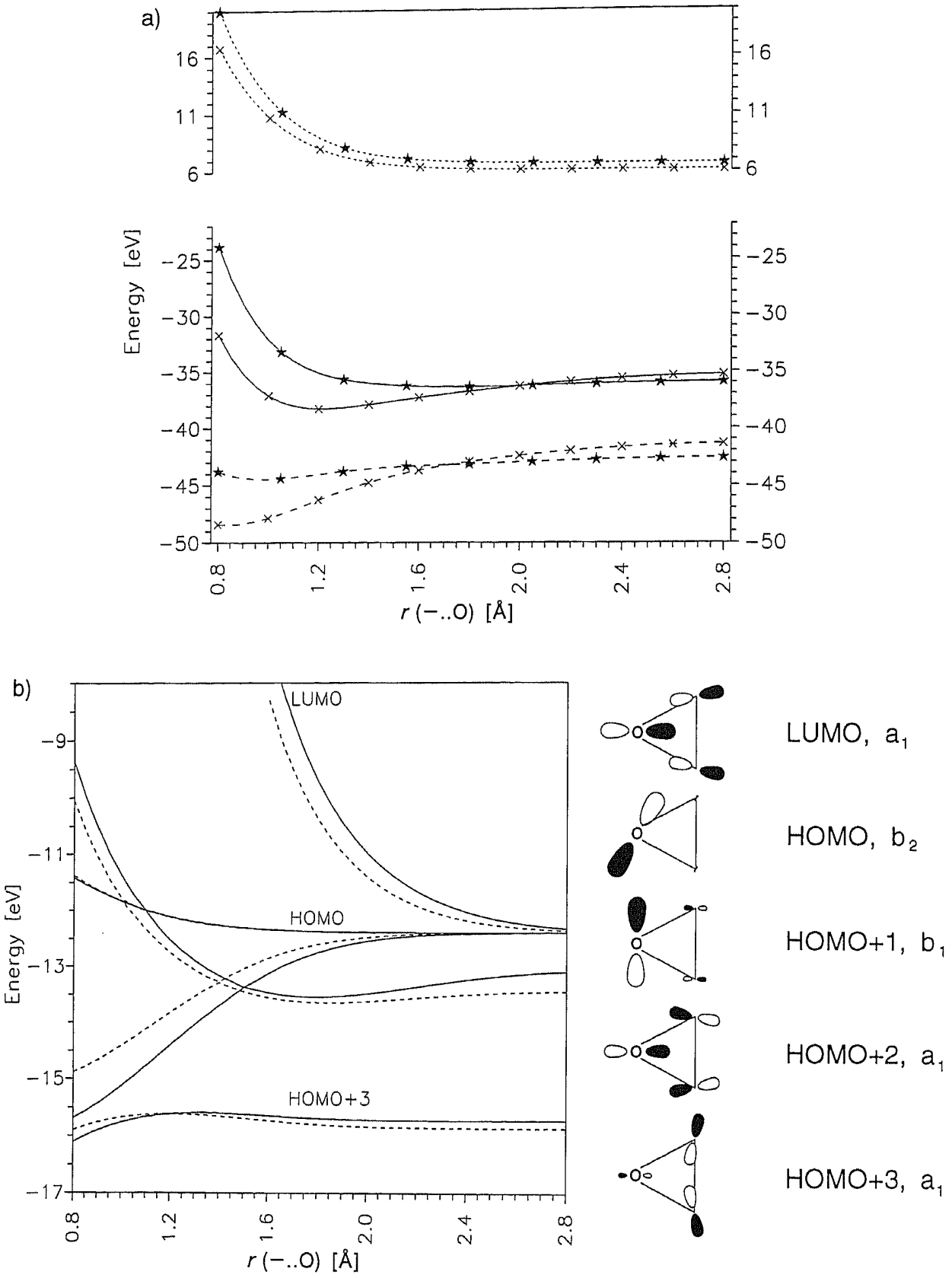

Fig. 11. *Influence of* κ *(C–O) on the* r *(–..O) stretching mode* **VIII** *of ethylene oxide. a)* (···): E_{Rep}, (——): E_{tot}, (----): ΔE_{EHMO}. The curves marked with a * have been calculated with κ (C–O) = 1.0 and a C–C distance of 1.42 Å. The curves marked with a x have been calculated with κ (C–O) = 1.2 and a C–C distance of 1.54 Å. *b)* Correlation diagram of the frontier orbitals from HOMO + 3 up to the LUMO. (----): κ (C–O) = 1.0, (——): κ (C–O) = 1.2. The wave functions on the right correspond to *r* (–.. O) = 1.70 Å.

Another approach discussed in the literature is the addition of a positive charge in form of a dummy proton in a position as indicated in **IX** [51]. We follow this second approach and study the influence of a proton of varying $E(H+) = H_{1s1s}$ at a distance $r(O-H^+)$ of 1.1 Å. Calculations have been carried out an angle Θ_1 of 0° because of the maximum overlap between the 1s AO and the oxygen lobe of the HOMO+2 at this angle. $\kappa(C-O) = 1.0$ was used and the repulsion term between the dummy proton and the epoxide was omitted. *Fig. 12* shows that withdrawal of charge from the HOMO+2 results in the expected shortening of the $r(-..O)$ distance which is, however, not sufficient to

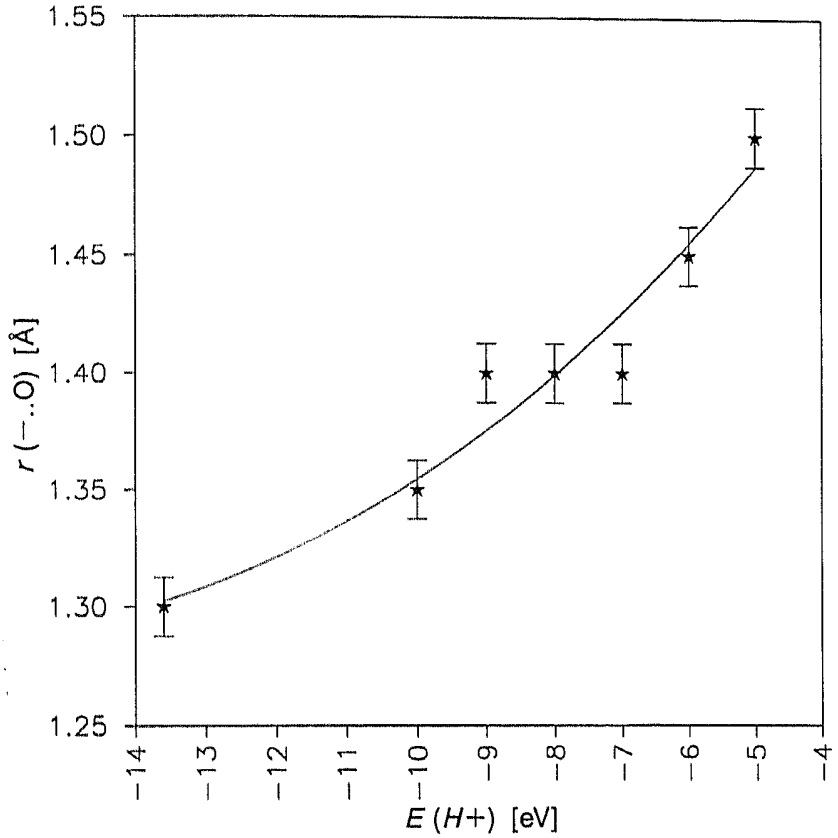

Fig. 12. *Protonated ethylene oxide.* Dependence of the minimum distance $r(-..O)$ on the *Coulomb* integral $E(H+) = H_{1s1s}$ of the proton. The calculated points have been interpolated by a quadratic function.

reach the experimental bond length. The same in a less pronounced form is observed, if calculations are carried out at an angle Θ_1 of 65°. This angle results by geometry optimization of the ethylene-oxide-proton adduct. It corresponds well to the one found with another procedure [51]. This means also that protonation of epoxide stabilizes the C–O bond. The charge of the C-atom remains nearly constant, whereas increasing charge transfer from the oxygen to the proton occurs when the 1s-level energy is decreased. To summarize, we can say that withdrawal of charge from the HOMO + 2 stabilizes r (C–O) by decreasing the antibonding interaction, while an increasing κ (C–O) leads to a stabilization of the HOMO + 1 by increasing the bonding interaction of this orbital.

6. Conclusion. – The extended-*Hückel* method in its improved ASED form has been examined by using geometry calculations on a number of hydrocarbons and on several organic molecules containing oxygen, nitrogen, and sulfur [52]. We have thoroughly investigated bond lengths and bond angles of aliphatic, conjugated and aromatic hydro-

carbons, and we have studied reaction enthalpies. As a general trend we found that bond lengths with an accuracy of 0.05 to 0.1 Å, and also bond angles can well be reproduced by a single set of (κ,δ) parameters. If, however, reaction enthalpies and more reliable geometries are of interest, the influence of sp, sp^2, sp^3 hybridization on κ must be taken into account. By splitting the total energy into atomic contributions, one can compare the stabilities of atoms in different molecular environments. The atomic contributions can be used for calculating bond energies by weighting them with the reduced atom-atom overlap populations. This has been tested for C–C, C=C, and C≡C bonds and also for C–H bonds in which the trend of increasing bond energy with increasing bond order is fulfilled. When we calculate O-, N-, and S-containing compounds with moderate contraction of the 2s-oxygen, the 2s-nitrogen, and the 3s-sulfur *Slater* exponents, we obtain good geometries for important classes of organic molecules. We have found that the geometries of the three membered rings $(CH_2)_2X$ (X = CH_2, NH, O, and S) which have attracted much interest and stimulated theoretical studies can be well reproduced. Despite of these encouraging results, one should not expect that very small tunnelling barriers as observed in ammonia, aniline and other cases can be calculated. Such double minimum problems are better discussed by, *e.g.*, introducing polarization functions in a second-order perturbation theory. It has been found that the EHMO method in its improved ASED form can be parametrized for organometallic molecules [53] to have at hand a semiempirical tool allowing rapid geometry optimization, and we have shown that the EHMO-ASED procedure can be successfully implemented in band-structure calculations [54]. Calculation of reliable geometries, however, demands careful investigation on the influence of the parameters.

Modern molecular mechanics allows to calculate molecular geometries of organic molecules with high accuracy [55]. As a supplement the extended-*Hückel* method in its improved ASED form can be regarded as a useful tool for combining the information of the EHMO results with good geometry calculations for many organic and inorganic molecules.

We would like to thank Dr. *K. Hädener* for helpful discussions, and *IBM*, Switzerland, for financial support. This work is part of project NF 2–5.542 financed by the *Schweizerischer Nationalfonds zur Förderung der wissenschaftlichen Forschung* and by project BBW-REN(88)28/EPA 217.307 financed by the *Schweizerisches Bundesamt für Energiewirtschaft*.

REFERENCES

[1] R. Hoffmann, W. N. Lipscomb, *J. Chem. Phys.* **1962,** *36,* 2179.
[2] a) R. Hoffmann, *J. Chem. Phys.* **1963,** *39,* 1397; b) *ibid.* **1964,** *40,* 2474; c) *ibid.* **1964,** *40,* 2745.
[3] R. B. Woodward, R. Hoffmann, *J. Am. Chem. Soc.* **1965,** *87,* 395, 2046, 2511, 4388, 4389.
[4] R. B. Woodward, R. Hoffmann, *Acc. Chem. Res.* **1968,** *1,* 17.
[5] R. Hoffmann, *Acc. Chem. Res.* **1971,** *4,* 1.
[6] R. Hoffmann, 'Pure and Applied Chemistry', Butterworths, London, 1991, Vol. 2, p. 235.
[7] L. Libit, R. Hoffmann, *J. Am. Chem. Soc.* **1974,** *96,* 1370.
[8] R. Hoffmann, H. Fujimoto, J. R. Swenson, C.-C. Wan, *J. Am. Chem. Soc.* **1973,** *95,* 7644.
[9] a) M. Elian, R. Hoffmann, *Inorg. Chem.* **1975,** *14,* 1058; b) R. Hoffmann, M. M.-L. Chen, D. L. Thorn, *ibid.* **1977,** *16,* 503; c) R. Hoffmann, *Angew. Chem.* **1982,** *94,* 725.
[10] a) M.-H. Whangbo, R. Hoffmann, *J. Am. Chem. Soc.* **1978,** *100,* 6093; b) R. Hoffmann, 'Solids and Surfaces: A Chemist's View of Bonding in Extended Structures', VCH, New York, 1988; c) R. Hoffmann, C. Janiak, C. Kollmar, *Macromolecules* **1991,** *24,* 3725.

[11] H. Basch, A. Viste, H. B. Gray, *Theor. Chim. Acta* **1965,** *3,* 458.
[12] C. J. Ballhausen, H. B. Gray, 'Molecular Orbital Theory', W. A. Benjamin, New York, 1965.
[13] R. Gleiter, *J. Chem. Soc. (A)* **1970,** 3174.
[14] R. Gleiter, *Angew. Chem.* **1974,** *86,* 770.
[15] K. F. Purcell, J. C. Kotz, 'Inorganic Chemistry', W. B. Saunders, New York, 1977.
[16] T. A. Albright, J. K. Burdett, M. H. Whangbo, 'Orbital Interaction in Chemistry', Wiley, New York, 1985.
[17] R. W. Grimes, D. Onwood, *J. Chem. Soc., Faraday Trans.* **1990,** *86,* 233.
[18] P. Siddarth, R. A. Marcus, *J. Phys. Chem.* **1990,** *94,* 2985.
[19] A. B. Anderson, R. Hoffmann, *J. Chem. Phys.* **1974,** *60,* 4271.
[20] a) A. B. Anderson, *J. Chem. Phys.* **1977,** *66,* 5108; b) A. B. Anderson, *Phys. Rev. B* **1977,** *16,* 900; c) A. B. Anderson, *J. Chem. Phys.* **1975,** *62,* 1187, *ibid.* **1978,** *68,* 1744; d) A. B. Anderson, R. W. Grimes, S. Y. Hong, *ibid.* **1987,** *91,* 4245; e) A. B. Anderson, S. Y. Hong, J. L. Smialek, *ibid.* **1987,** *91,* 4250.
[21] a) G. Calzaferri, L. Forss, I. Kamber, *J. Phys. Chem.* **1989,** *93,* 5366; b) G. Calzaferri, *Chimia* **1986,** *40,* 74.
[22] G. Calzaferri, R. Hoffmann, *J. Chem. Soc., Dalton Trans.* **1991,** 917.
[23] E. Amouyal, M. Mouallem-Bahout, G. Calzaferri, *J. Phys. Chem.* **1991,** *95,* 7641.
[24] S. Bergamasco, G. Calzaferri, K. Hädener, *J. Photochem. Photobiol. A: Chem.* **1992,** *66,* 327.
[25] R. S. Mulliken, *J. Phys. Chem.* **1955,** *23,* 1833, 1841.
[26] M. Wolfsberg, L. Helmholz, *J. Chem. Phys.* **1952,** *20,* 837.
[27] J. H. Ammeter, H. B. Bürgi, J. C. Thibeault, R. Hoffmann, *J. Am. Chem. Soc.* **1978,** *100,* 3686.
[28] 'Landolt-Börnstein Zahlenwerte und Funktionen aus Naturwissenschaften und Technik, Neue Serie, Gruppe 2, Atom- und Molekularphysik', Springer-Verlag, Berlin, 1976, Vol. 7.
[29] H. A. Jahn, E. Teller, *Proc. R. Soc. London. [Ser.] A* **1937,** *161,* 220.
[30] D. R. Lide, Jr., *J. Chem. Phys.* **1958,** *29,* 1426.
[31] H. Irngartinger, M. Nixdorf, N. H. Riegler, A. Krebs, H. Kimling, J. Pocklington, G. Maier, K.-D. Malsch, K.-A. Schneider, *Chem. Ber.* **1988,** *121,* 673.
[32] W. Caminati, B. Vogelsanger, A. Bauder, *J. Mol. Spectrosc.* **1988,** *128,* 384.
[33] M. Traetteberg, E. B. Frantsen, F. C. Mijlhoff, A. Hoeckstra, *J. Mol. Struct.* **1975,** *26,* 57.
[34] L. A. Carreira, *J. Chem. Phys.* **1975,** *62,* 3851.
[35] F. Momicchioli, I. Baraldi, M. C. Bruni, *Chem. Phys.* **1983,** *82,* 229.
[36] F. Momicchioli, I. Baraldi, M. C. Bruni, *Chem. Phys.* **1982,** *70,* 161.
[37] U. Pincelli, B. Cadioli, B. Lévy, *Chem. Phys. Lett.* **1972,** *13,* 249.
[38] R. R. Hautala, R. B. King, C. Kutal, Eds., 'Solar Energy – Chemical Conversion and Storage', Humana, Clifton, N.Y., 1979, p. 339.
[39] C. Philippopoulos, J. Marangozis, *Ind. Eng. Chem. Prod. Res. Dev.* **1984,** *23,* 458.
[40] I.-F. Duan, C.-H. Cheng, J.-S. Shaw, S.-S. Cheng, K. F. Liou, *J. Chem. Soc., Chem. Commun.* **1991,** 1347.
[41] S. W. Benson, 'Thermochemical Kinetics – Methods for the Estimation of Thermochemical Data and Rate Parameters', 2nd edn., J. Wiley & Sons, New York, 1976.
[42] P. W. Atkins, 'Physical Chemistry', 4th edn., Oxford University Press, Oxford, 1991, p. 939.
[43] W. Kutzelnigg, 'Einführung in die Theoretische Chemie, Band 2: Die chemische Bindung', Verlag Chemie, Weinheim–New York, 1978.
[44] J. C. Slater, *Phys. Rev.* **1930,** *36,* 57.
[45] S. J. Cyvine, 'Molecular Vibrations and Means Square Amplitudes', Elsevier, Amsterdam, 1968.
[46] A. Rauk, L. C. Allen, E. Clementi, *J. Chem. Phys.* **1970,** *52,* 4133.
[47] A. D. Buckingham, E. Lippert, S. Bratos, 'Organic Liquids, Structure, Dynamics, and Chemical Properties', John Wiley & Sons, New York, 1978, p. 175.
[48] R. Gleiter, *Topics Curr. Chem.* **1979,** *86,* 197.
[49] E. Honegger, E. Heilbronner, A. Schmelzer, *Nouv. J. Chim.* **1982,** *6,* 519.
[50] M. J. Calhorda, R. Hoffmann, C. M. Friend, *J. Am. Chem. Soc.* **1990,** *112,* 50.
[51] H. Fujimoto, R. Hoffmann, *J. Phys. Chem.* **1974,** *78,* 1874.
[52] A computer program to perform EHMO-ASED calculations is available from QCPE: G. Calzaferri, M. Brändle, QCMP No. 116, QCPE Bulletin, Vol. 12, No. 4, 1992.
[53] F. Savary, J. Weber, G. Calzaferri, *J. Phys. Chem.* **1993,** in press.
[54] M. Brändle, G. Calzaferri, submitted.
[55] J. C. Smith, M. Karplus, *J. Am. Chem. Soc.* **1992,** *114,* 801.